Beni-Suef University Journal of Basic and Applied Sciences

RESEARCH

Open Access

In silico profiling of histone deacetylase inhibitory activity of compounds isolated from *Cajanus cajan*

Kayode Adewole[1], Adebayo Ishola[2] and Ige Olaoye[2,3*]

Abstract

Background: Cancer is responsible for high morbidity and mortality globally. Because the overexpression of histone deacetylases (HDACs) is one of the molecular mechanisms associated with the development and progression of some diseases such as cancer, studies are now considering inhibition of HDAC as a strategy for the treatment of cancer. In this study, a receptor-based in silico screening was exploited to identify potential HDAC inhibitors among the compounds isolated from *Cajanus cajan*, since reports have earlier confirmed the antiproliferative properties of compounds isolated from this plant.

Results: *Cajanus cajan*-derived phytochemicals were docked with selected HDACs, with givinostat as the reference HDAC inhibitor, using AutodockVina and Discovery Studio Visualizer, BIOVIA, 2020. Furthermore, absorption, distribution, metabolism and excretion (ADME) drug-likeness analysis was done using the Swiss online ADME web tool. From the results obtained, 4 compounds; betulinic acid, genistin, orientin and vitexin, were identified as potential inhibitors of the selected HDACs, while only 3 compounds (betulinic acid, genistin and vitexin) passed the filter of drug-likeness. The molecular dynamic result revealed the best level of flexibility on HDAC1 and HDAC3 compared to the wild-type HDACs and moderate flexibility of HDAC7 and HDAC8.

Conclusions: The results of molecular docking, pharmacokinetics and molecular dynamics revealed that betulinic acid might be a suitable HDAC inhibitor worthy of further investigation in order to be used for regulating conditions associated with overexpression of HDACs. This knowledge can be used to guide experimental investigation on *Cajanus cajan*-derived compounds as potential HDAC inhibitors.

Keywords: *Cajanus cajan*, Molecular docking, ADME, Histone deacetylase, Histone deacetylase inhibitor

1 Background

There is an increasing interest in the consumption of functional foods since it is believed that beyond supplying the body's basic nutrients, functional foods also contain bioactive compounds that could be therapeutically beneficial to the body [1, 2]. Among plant foods that have attracted interest as a functional food is *Cajanus cajan* (pigeon pea) because of its popularity in the ethnomedicine of Africa, Central America, India and many other countries [3]. *Cajanus cajan* seed is very rich in proteins, carbohydrates, minerals, vitamins, and essential amino acids [3, 4]. This plant is an important food in many parts of the world where the leaves are also eaten fresh in salads or as a blanched vegetable. *Cajanus cajan* is used in traditional medicine in some countries for the treatment of various diseases like bed sores, measles, oral ulcers, diabetes, dysentery, genital irritations, hepatitis, menstrual disorders and urinary tract infections [5, 6]. Some of these traditional claims have been scientifically evaluated. For instance, different studies

*Correspondence: igeolarinoye@gmail.com
[2] Central Research Laboratories Limited, 132B University Road Ilorin, Ilorin, Nigeria
Full list of author information is available at the end of the article

have reported that extracts and compounds isolated from *C. cajan* possess antiinflammatory, antioxidative, antibacterial, hypoglycemic, hypocholesterolemic and antiproliferative effects [3, 7, 8]. Such studies have reported the antiproliferative effects of *C. cajan* extracts and its bioactive compounds on different cancer cell lines, including human breast adenocarcinoma (MCF-7), human cervical adenocarcinoma (HeLa), human colorectal adenocarcinoma (Caco-2), human lung cancer (A549), and human hepatoma (HepG2) cells [3, 8–10, 12]. From these studies, some of the mechanisms of anticancer action have been identified. Specific examples include induction of apoptosis, arrest of cell cycle in the G2/M phase, upregulation of Bax, downregulation of Bcl-2, activation of caspase-3, induction BRCA-related DNA damage in breast cancer cells, and binding and inhibiting estrogen receptor alpha (ERα) in ERα-positive breast cancer cells by cajaninstilbene acid [10, 11]. Other examples include arrest of cell cycle at G2/M phase, induction of apoptosis through reactive oxygen species-mediated mitochondria-dependent pathway in breast cancer cells by cajanol [8], modulation of the activity of peroxisome proliferator-activated receptor gamma by ethanolic extract of C. cajan leaf which have orientin, pinostrobin, vitexin, cajaninstilbene acid, and pinosylvin monomethylether as the major active compounds [3]. The cytotoxicity of cajanstilbenoids A against human hepatoma, human breast adenocarcinoma, and human lung cancer cells, as well as the cytotoxicity of cajanstilbenoids B against human hepatoma have also been reported [12]. These studies suggest the anticancer potential, as well as the anticancer mechanisms of compounds isolated from *C. cajan*. While the delicate control of cell cycle is a crucial regulatory apparatus of cell growth, making the blockade of cell cycle a very useful strategy in anticancer drug development [13], induction of the mitochondria-dependent apoptotic pathway, as well as modulation of the activity of peroxisome proliferator-activated receptor gamma are also strategies in the development of novel anticancer therapies [14, 15]. However, some other important anticancer mechanisms are yet to be evaluated. One of such is the epigenetic modification of DNA by histone deacetylases (HDACs), an important factor in the etiology of some cancers such as breast cancer, T-cell lymphoma, and multiple myeloma [16–18]. HDACs catalyze one of the most common events in post-translational modifications; the removal of acetyl group from N-terminal lysine side chain of histone and non-histone proteins. However, studies have shown that DNA methylation and posttranslational histone modifications are dysregulated in human cancer cells, with the serious consequence on gene transcription [19]. Specific examples are seen in the regulation of cell cycle by HDACs 1, and 3, over expression of HDAC1 in gastric, breast, prostate and colon cancers [20, 21], over expression of HDAC2 in gastric, cervical and colorectal cancers [22, 23], overexpression of HDAC3 in colon cancer [21], over activities of HDAC2 and HDAC3 in breast tumors [24], over expression of HDAC8 in childhood neuroblastoma [25] as well as the involvement of HDAC1 and HDAC8 in breast cancer metastasis [17].

Overexpression of HDACs in the formation and progression of some cancers have therefore made them targets in the development of novel anticancer drug. This involves development of HDAC inhibitors (HDIs) which bind and inhibit the activity and overexpression of target HDACs, as exemplified by the downregulation in the expression of HDAC7 by apicidin in salivary mucoepidermoid carcinoma cells [26]. Therefore, targeting HDACs with inhibitors is a major strategy in anticancer drug research and discovery. The approval of some HDIs by the Food and Drug Administration for the treatment of some cancers has generated more interest in finding new HDIs as anticancer agents in the continuous search for new anticancer drugs. However, synthetic HDIs have been shown to have some undesirable side effects including anorexia, dehydration, diarrhoea, dehydration, fatigue and nausea [27, 28]. It is therefore rational to look for new HDIs from natural sources as better substitutes for the synthetic ones. This approach has resulted in the identification of some HDIs, such as apigenin [29], luteolin [30], apicidin [26], curcumin [31], linoleic acid, stigmasterol and sulforaphane from plant sources [32] with some of these compounds at different stages of drug development. Therefore, to identify new HDIs as potential agents for anticancer drug development, compounds isolated from *C. cajan* were screened for HDAC inhibitory potentials using in silico methods. This is to evaluate whether *C. cajan*-derived compounds exhibit similar interaction profile with givinostat (a known standard HDAC inhibitor) based on earlier reports of their antiproliferative activity. The critical active site residues contributing significantly toward the stability of these compounds at the binding pockets of the selected HDACs were also evaluated, while compounds with significant histone deacetylase inhibitory activity, based on their binding affinities with the selected HDACs relative to givinostat were further subjected to Absorption Distribution Metabolism and Excretion (ADME) drugability test as outlined by Lipinski rule of

5. The results and insights from this study could support further studies on *C. cajan*-derived compounds and the possibility of using these compounds as therapies against abnormalities linked with over activity of the selected HDAC isoforms.

2 Methods

2.1 Protein preparation

The crystal structures of HDAC1, HDAC3, HDAC7 and HDAC8 (with PDB IDs 4BKX, 4A69, 3C10 and 5FCW respectively) were retrieved from the protein databank (www.rcsb.org) [33]. All the crystal structures were prepared individually by removing existing ligands and water molecules while missing hydrogen atoms were added using Autodock v4.2 program, Scripps Research Institute. Thereafter, non-polar hydrogens were merged while polar hydrogen where added to each enzyme. The process was repeated for each HDAC and subsequently saved into dockable pdbqt format in preparation for molecular docking.

2.2 Ligand preparation

SDF structures of givinostat, trichostatin A (standard HDAC inhibitors) and those of 13 phytochemical ligands derived from *C. cajan* (2-hydroxygenistein, betulinic acid, biochanin A, cajaninstilbene acid, cajanol, cajanuslactone, genistein, genistin, longistylin A, longistylin C, orientin, pinostrobin, vitexin), were retrieved from the PubChem database (www.pubchem.ncbi.nlm.nih.gov) [34]. The compounds were converted to mol2 chemical format using Open babel [35]. Polar hydrogens were added while non polar hydrogens were merged with the carbons and the internal degrees of freedom and torsions were set. The protein and ligand molecules were further converted to the dockable pdbqt format using Autodock tools.

2.3 Molecular docking

Docking of the ligands to various protein targets and determination of binding affinities was carried out using Vina [36]. Pdbqt format of HDACs and ligands were dragged into their respective columns. The grid center for docking was detected as $X = -62.66$, $Y = 17.19$, $Z = -4.97$ with the dimension of the grid box $72.96 \times 76.12 \times 66.09$ for HDAC1, $X = 24.12$, $Y = 58.49$, $Z = 22.64$ with the dimension of the grid box $99.81 \times 91.84 \times 64.94$ for HDAC3, $X = -3.08$, $Y = 2.52$, $Z = 0.05$ with the dimension of the grid box $56.51 \times 58.25 \times 70.89$ for HDAC7, $X = 40.18$, $Y = 16.13$, $Z = 118.20$ with the dimension of the grid box $72.18 \times 91.64 \times 78.49$ for HDAC8. Subsequently the software was run and a cluster analysis based on root mean square deviation (RMSD) values, with reference to the starting geometry was performed and the lowest energy conformation of the more populated cluster was considered as the most trustable solution. The binding affinities of compounds for the 4 HDAC isoforms targets were recorded. The compounds were then ranked by their affinity scores. For the sake of comparison of in silico performance, the molecular interactions between HDACs and compounds with binding affinity equal or greater than standard inhibitor (givinostat) were viewed with Discovery Studio Visualizer, BIOVIA, 2020.

2.4 Molecular dynamics (MD) simulations

To predict the stability of HDAC1, 3, 7, and 8 complexes, molecular dynamics simulations (MDS) were performed in GROMACS 2020.5 [37]. The MDS were executed on a work station with configuration; Ubuntu 20.04 LTS 64-bit, 16 GB RAM, Intel ®CoreTM i7-9750H CPU with 4 gigabyte dedicated NVIDIA GeForce graphics card. Each ligand was processed by converting the docked file to mol2 format by using the Avogadro program [38], which was then used to prepare the.STR file using the CGenFF server. After that, using the cgenff_charmm2gmx.py python script, the STR file was used to prepare the top, prm and lig_ini file using CHARMM 36 force field [39]. The resulting lig_ini file was used to prepare the gro file of the ligand g_editconf module. Thereafter ligand topologies were rejoined to the processed protein structure for building the complex system. Also, CHARMM 36 force field for preparing the gro file for protein and topol file by using g_pdb2gmx module in GROMACS. Thereafter, ligand topologies were rejoined to the processed protein structures for building the complex system. A water solvated system was built by using the TIP3P water model with dodecahedral periodic boundary conditions. Each solvated system was neutralized by the addition of Na^+ Cl^- ions. Energy minimization was done at 10 $KJmol^{-1}$ with steepest descent Algorithm by using the Verlet cut-off scheme taking Particle Mesh Edward (PME) Coulombic interactions with a maximum of 50,000 steps. Equilibration of the system was obtained in two steps. Firstly, NVT equilibration was done in 300 K and 5000 ps of steps, while in the second step, NPT equilibration taking Parrinello-Rahman (pressure coupling), 1 bar reference pressure, and 5000 ps of steps. To evaluate the result, the simulation trajectory was saved for every 100 ps. The simulation results were incorporated with the GROMACS default script. Finally, MD trajectories were evaluated for the measurement of Root-mean-square-deviation

(RMSD), Root mean square-fluctuation (RMSF), Radius of gyration (Rg), Hydrogen bonds (H-bonds) and Solvent Accessible Surface Area (SASA). This was worked out to measure the strength of the protein–ligand interaction. In order to get a more accurate MD simulation result, each complex was run three times (n = 3) and the average result was used for analysis.

2.5 Binding free energy calculation using MM-PBSA

The binding free energy, including the free solvation energy (polar and nonpolar solvation energies) and potential energy (electrostatic and Vander Waals interactions) of each protein–ligand complex were calculated by the Molecular Mechanics Poisson–Boltzmann Surface Area (MM-PBSA) method. The MD trajectories were processed before MM-PBSA calculations for 10 ns. The MM-PBSA binding free energy calculation was done with 'g_mmpbsa' [40] (Kumari et al., 2014) script. The binding energy was calculated by using the following equation:

$$\Delta Gbinding = \Delta Gcomplex - (\Delta Greceptor - \Delta Gligand)$$

where: ΔG binding = the total binding energy of the complex, ΔG receptor = the binding energy of free receptor, ΔG ligand = the binding energy of unbounded ligand.

2.6 Druglikeness and prediction of ADME

In silico methods for the determination of absorption, distribution, metabolism, and excretion (ADME) parameters depends on theoretically derived statistical models, which have been generated by relating the structural characteristics of compounds that have been measured in a given assay to their biological responses and is now widely used due to its low resource requirement [41]. Therefore, compounds that exhibited equal or higher binding affinity for at least one of the five HDACs were evaluated for their ADME properties (drug likeness) using the Swiss online ADME web tool [42–44].

3 Results

The binding affinities obtained from the molecular docking of the 13 *C. cajan* derived-compounds revealed that four compounds have higher binding affinities for HDAC1 and HDAC 3 relative to the standard inhibitor, givinostat, with the values indicated in bold values (Table 1). The binding affinities of the four compounds; betulinic acid, genistin, orientin and vitexin for HDAC1 are 15.4 kcal/mol, 13.4 kcal/mol, 12.6 kcal/mol and 12.3 kcal/mol respectively compared to 11.9 kcal/mol for givinostat (Table 1). For HDAC3, the binding affinities of the four compounds are −14.8 kcal/mol, −13.4 kcal/mol, −13.4 kcal/mol, −13.6 kcal/mol compared to −13.3 kcal/mol for givinostat (Table 1). However, only two out of the 13 compounds i.e. betulinic acid, and orientin displayed higher binding affinity of −15.9 kcal/mol, −13.6 kcal/mol respectively for HDAC8 compared to −13.4 kcal/mol for givinostat (Table 1), while two compounds i.e. betulinic acid, and genistin also have a more negative or equal binding affinity of −15.8 kcal/mol, and −14.0 kcal/mol for HDAC7 compared to 14.0 kcal/mol for the standard inhibitor (Table 1).

Table 1 Binding affinity of *Cajanus cajan* derived compounds to HDAC1, HDAC3, HDAC8 and HDAC7

S/N	Compounds	Binding affinity (Kcal/mol)			
		HDAC1	HDAC3	HDAC8	HDAC7
S	**Givinostat (inhibitor)**	−11.9	−13.3	−13.4	−14.0
S	Trichostatin A **(inhibitor)**	−10.9	−12.8	−10.1	−11.8
1	2-hydroxygenistein	−10.5	−10.8	−10.0	−10.8
2	Betulinic acid	**−15.4**	**−14.8**	**−15.9**	**−15.8**
3	Biochanin A	−10.6	−10.2	−10.1	−11.2
4	Cajaninstilbene acid	−10.2	−11.1	−9.7	−10.0
5	Cajanol	−10.9	−10.9	−10.3	−11.1
6	Cajanuslactone	−11.2	−11.0	−11.8	−10.9
7	Genistein	−10.3	−10.2	−10.1	−10.4
8	Genistin	**−13.4**	**−13.4**	−12.7	**−14.0**
9	Longistylin A	−11.2	−11.0	−11.9	−10.9
10	Longistylin C	−10.9	−11.1	−10.8	−10.3
11	Orientin	**−12.6**	**−13.4**	**−13.6**	−13.4
12	Pinostrobin	−10.5	−10.5	−10.2	−11.0
13	Vitexin	**−12.3**	**−13.6**	−13.0	−13.2

Bold indicates phytocompounds from *C. cajan* with binding scores greater HDAC known inhibitor (Givinostat)

Givinostat binds to HDAC1 pocket consisting of TYR15, HIS39, ARG55, TYR333, ASP332, VAL198, ARG36, ASP16, GLY17, MET329, PHE25 and LYS260 (Fig. 1a) having hydrogen bond interaction with ASN40, ASP248 and ILE249 (Fig. 2a), while betulinic acid interacted via hydrogen bond with GLU287 and hydrophobic interactions (π-alkyl) with TYR15, ARG36, HIS39, and PHE252 (Fig. 2b) in the same binding pocket (Fig. 1b). Conventional hydrogen bond was predominant in the interaction between genistin and ASN40, THR196 and ASP256 of HDAC1 (Fig. 1c and 2c). Orientin, and vitexin occupy similar binding site in HDAC1 (Figs. 1d and 1e) with both having a hydrogen bond interaction with ARG residues at positions 36 and 55. However, vitexin had three hydrophobic interactions with TYR15, ARG55 and VAL198 (Fig. 2e) which was not found in orientin's binding mode (Fig. 2d).

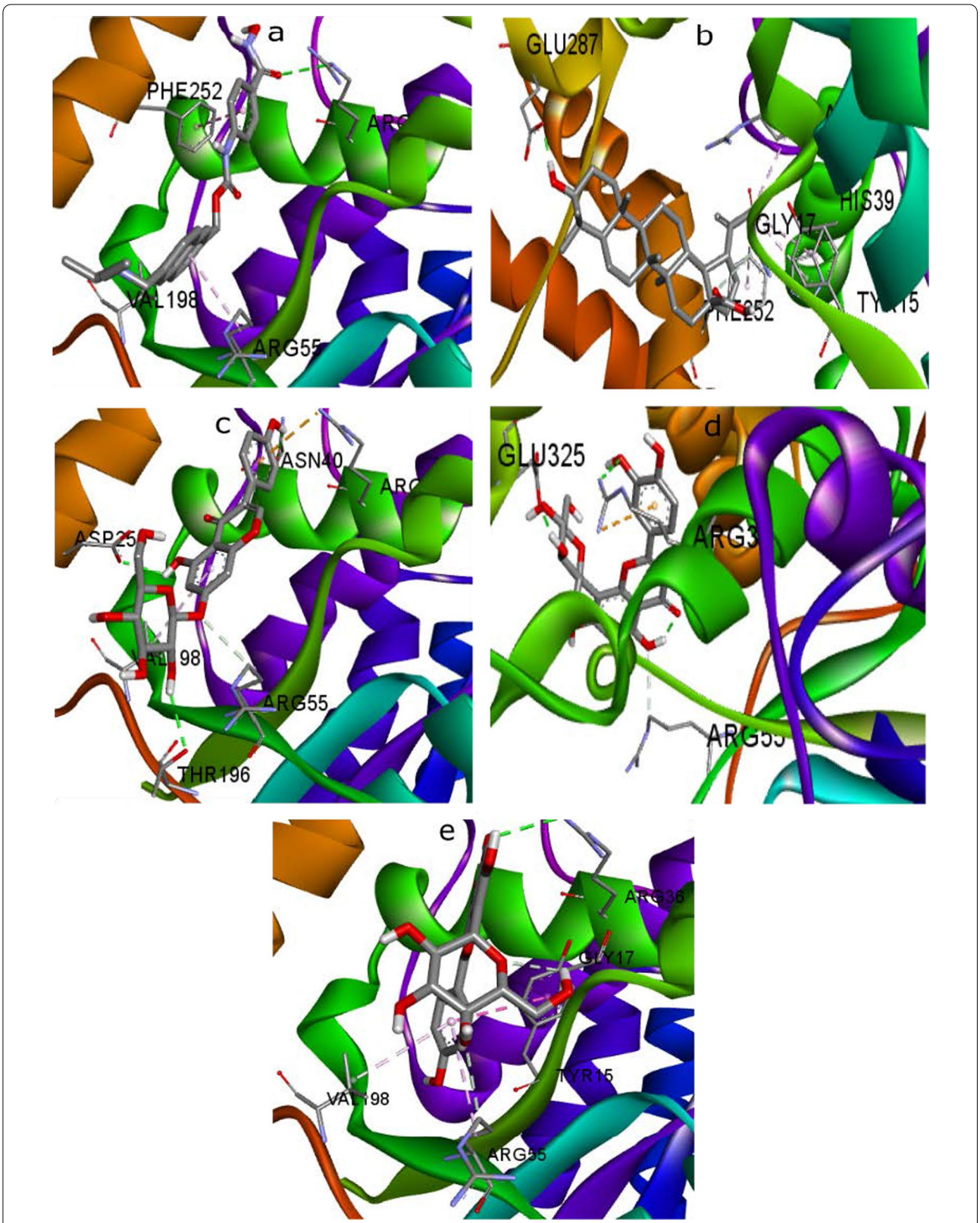

Fig. 1 3D view of the interaction between **a** givinostat **b** betulinic acid **c** genistin **d** orientin **e** vitexin and the binding sites in histone deacetylase 1

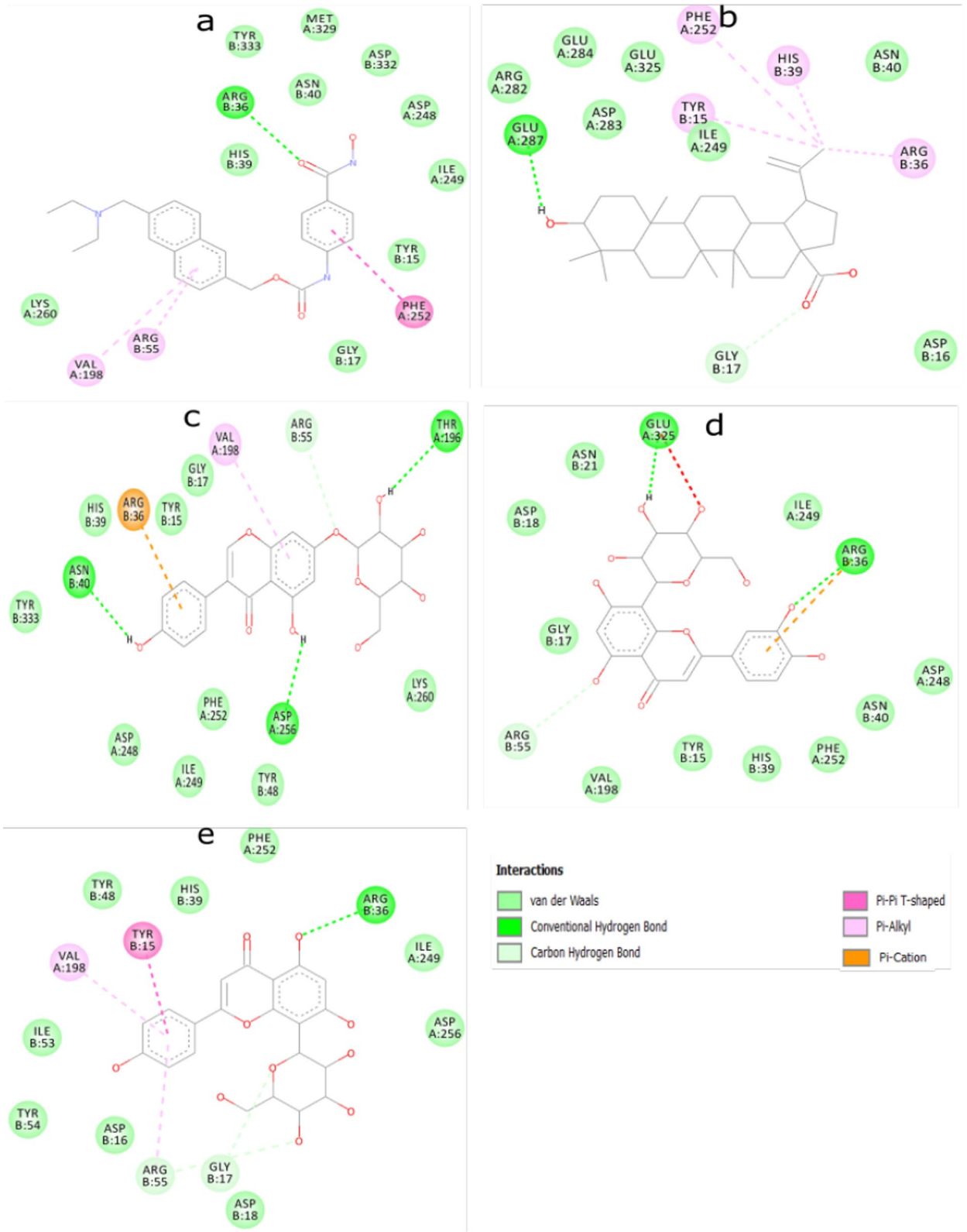

Fig. 2 2D view of the interaction between **a** givinostat **b** betulinic acid **c** genistin **d** orientin **e** vitexin and amino acids in the binding sites in histone deacetylase 1

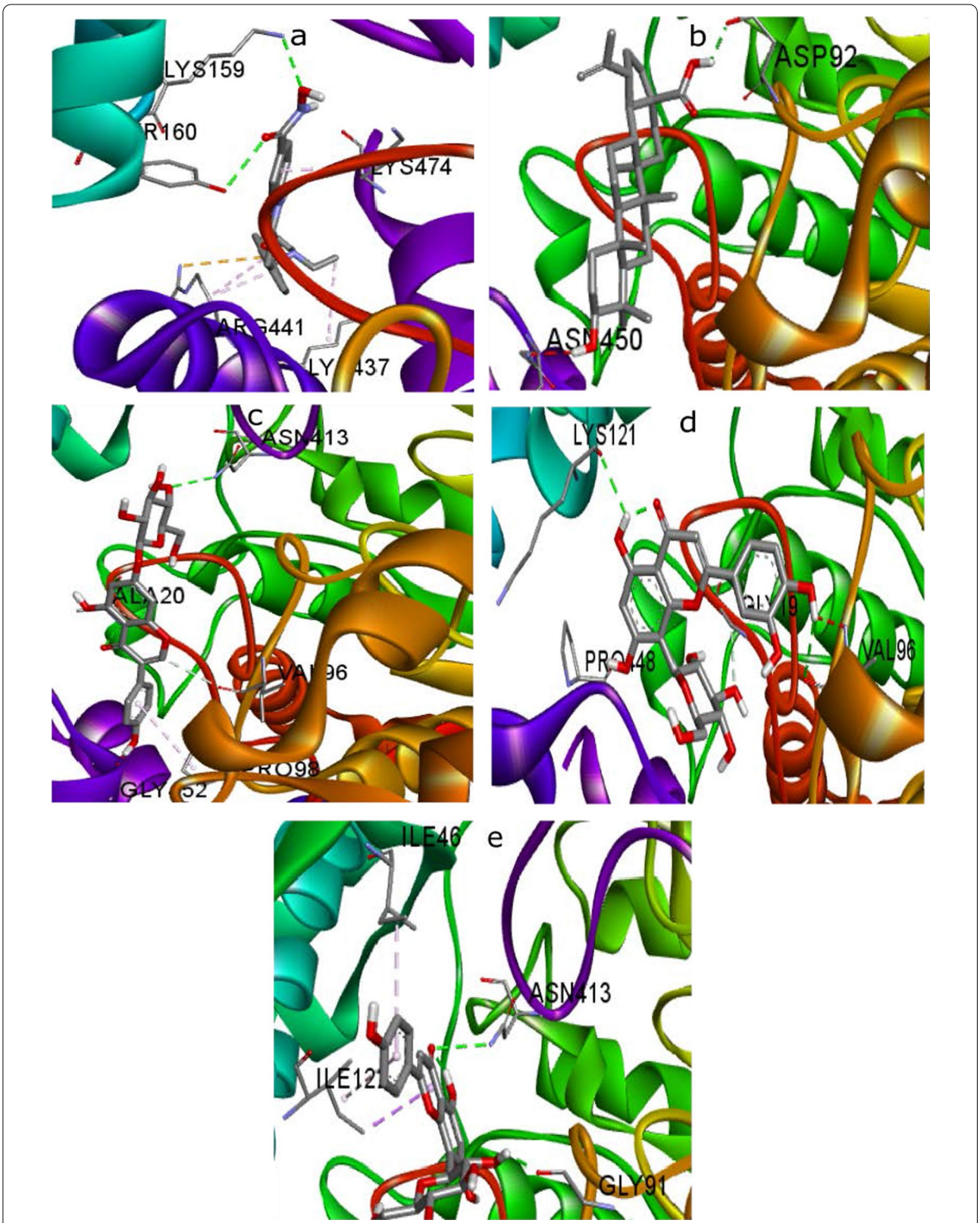

Fig. 3 3D view of the interaction between **a** givinostat **b** betulinic acid **c** genistin **d** orientin **e** vitexin and the binding sites in histone deacetylase 1

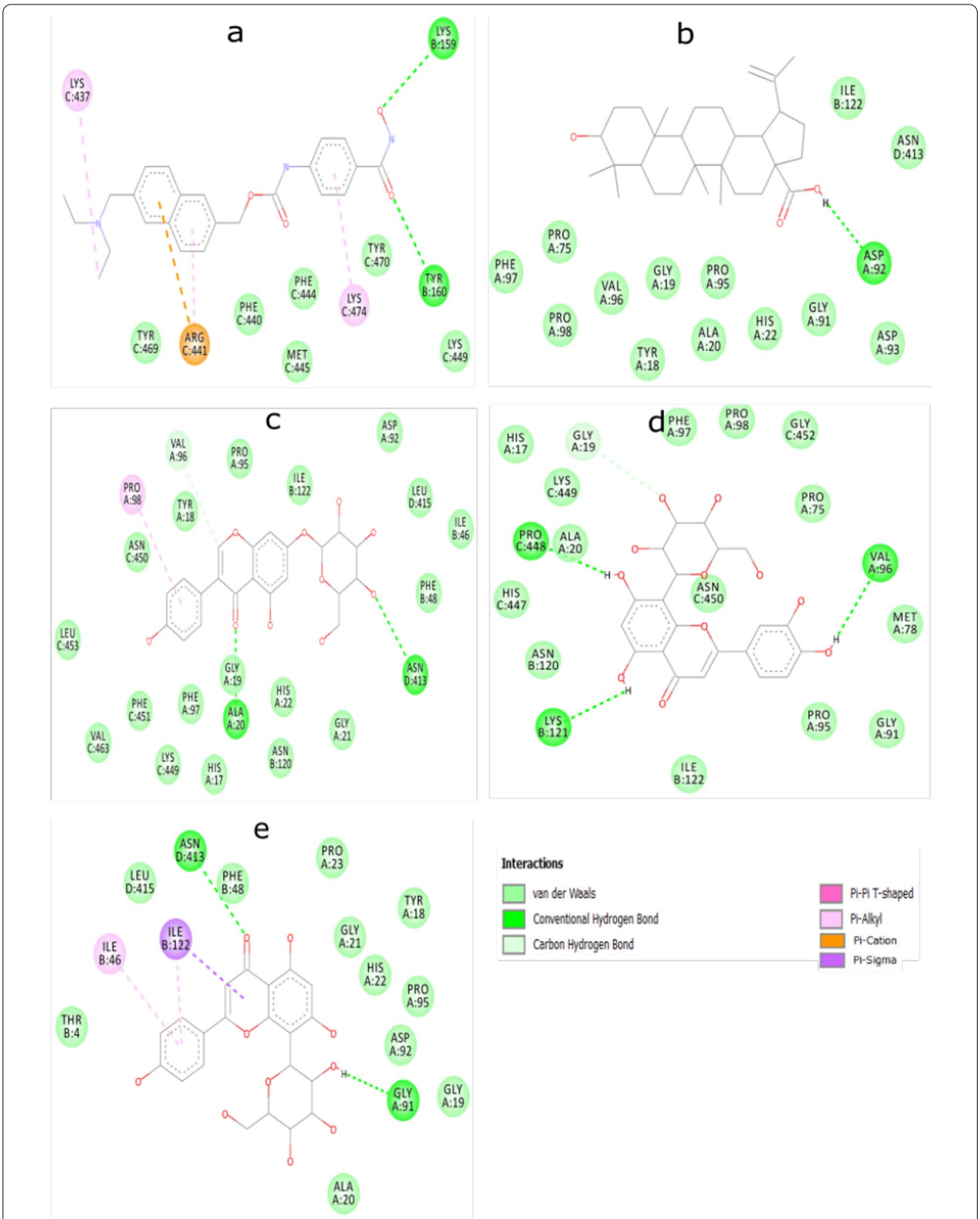

Fig. 4 2D view of the interaction between **a** givinostat **b** betulinic acid **c** genistin **d** orientin **e** vitexin and amino acids in the binding sites in histone deacetylase 3

Givinostat binding pocket in HDCA3 consist of residues LYS437, LYS159, THR469, TYR470, TYR160, MET445, LYS449, PHE444, PHE440, ARG441 (Fig. 3a). In addition to two hydrogen bond formed with LYS159 and TYR160, givinostat bind to HDAC3 via hydrophobic interactions with LYS437, ARG441, and LYS474 (Fig. 4a). Betulinic acid binds to a separate binding site in HDAC3 (Fig. 3b) with a single hydrogen bond formation with ASP92 (Fig. 4b). Genistin formed two hydrogen bonds with ALA20 and ASN413 in addition to hydrophobic interaction with PRO98 (Fig. 4c). Hydrogen bond formation (with GLY19, VAL96, LYS121, and PRO448) was the only means of interaction visualized in orientin's binding to HDAC3 (Fig. 4d). Vitexin interacted with HDAC3 via hydrogen bond formation with GLY91, and ASN413, in addition to hydrophobic interaction with two ILE residues at positions 46 and 122 (Fig. 4e).

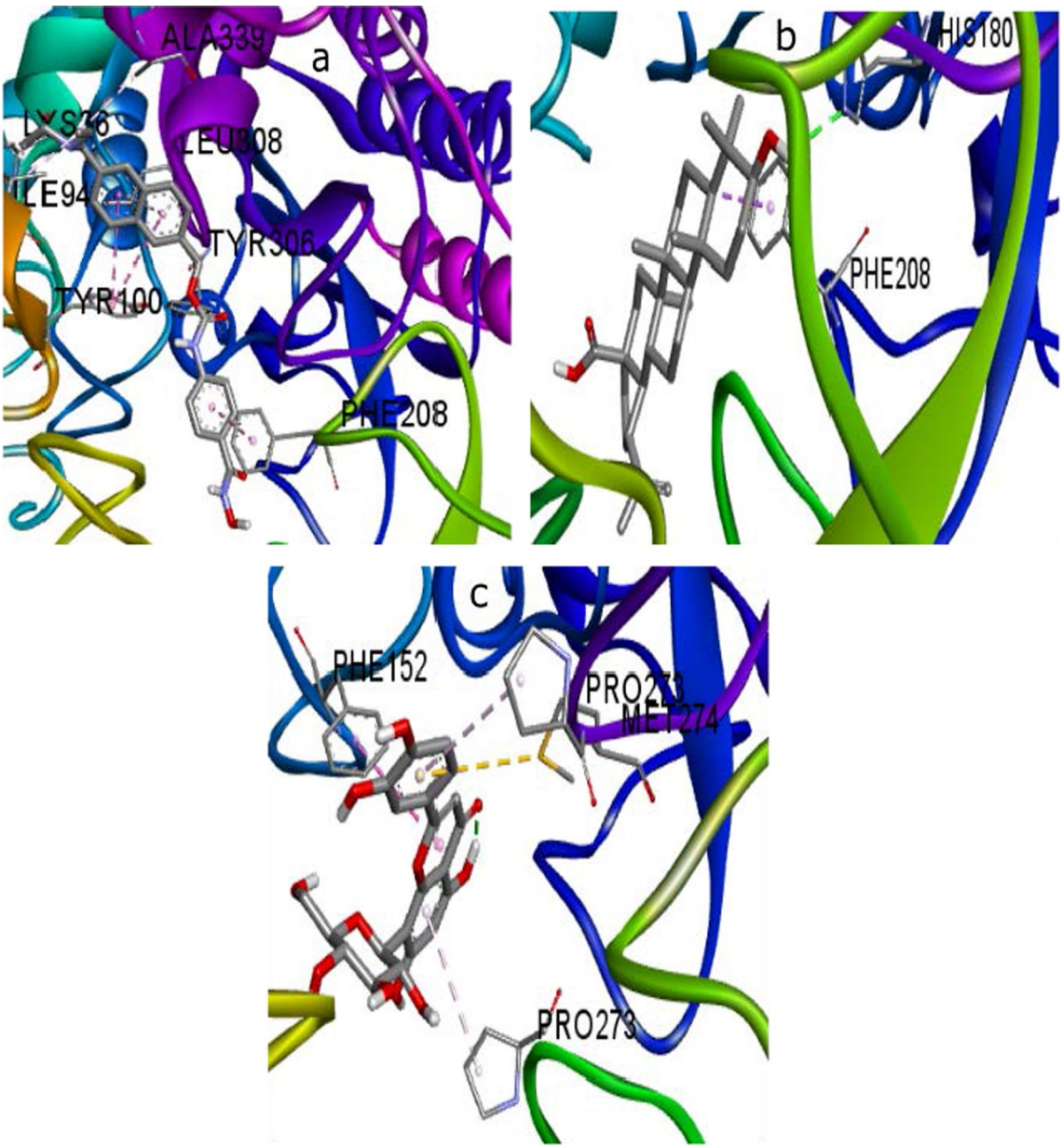

Fig. 5 3D view of the interaction between **a** givinostat **b** betulinic acid **c** orientin and the binding sites in histone deacetylase 8

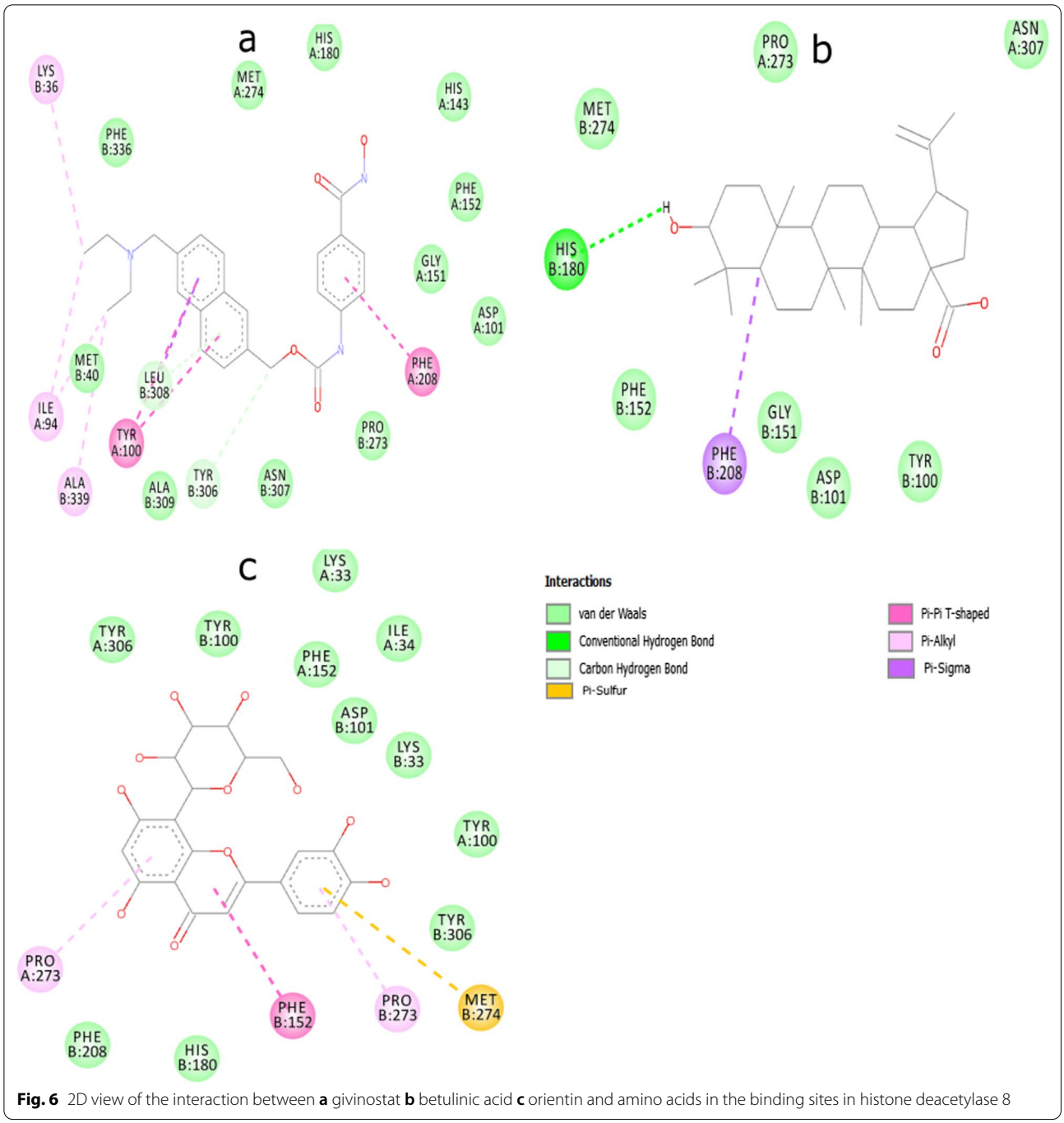

Fig. 6 2D view of the interaction between **a** givinostat **b** betulinic acid **c** orientin and amino acids in the binding sites in histone deacetylase 8

Similar binding pocket in HDAC8 was occupied by givinostat, betulinic acid and orientin in HDAC8 (Fig. 5). Hydrophobic interaction was the predominant mode of interaction between betulinic acid and HDAC8 (Fig. 6a). A single hydrogen bond (with HIS180) and a single π-sigma interaction (with PHE208) were the only bonds formed between betulinic acid and HDAC8 (Fig. 6b) while a π-sulphur interaction was observed between orientin and HDAC8 (Fig. 7c).

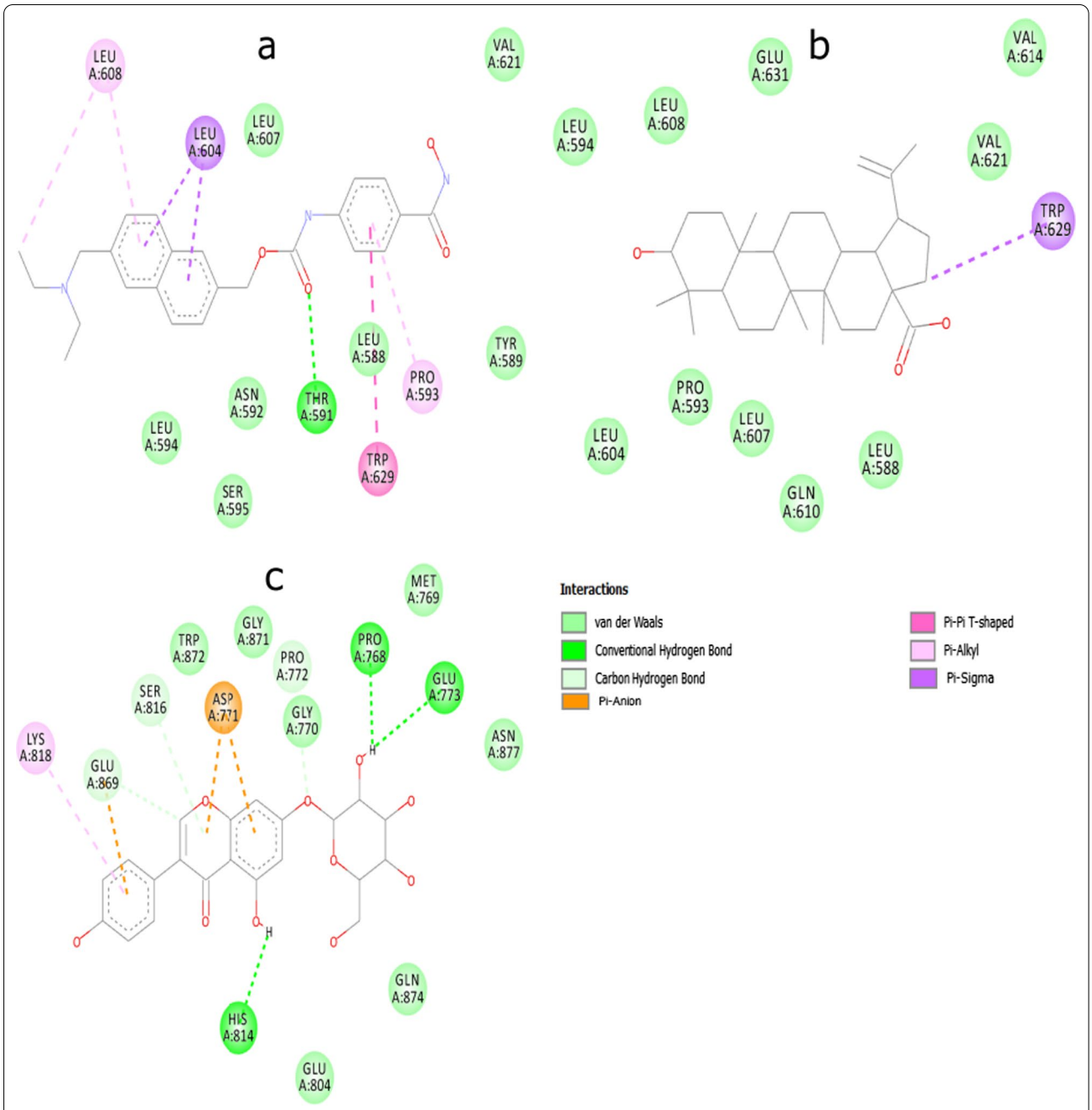

Fig. 7 2D view of the interaction between **a** givinostat **b** betulinic acid **c** orientin and amino acids in the binding sites in histone deacetylase 8

Givinostat and betulinic acid occupied similar binding pocket formed majorly by TRP629, and LEU residues at positions 604, 607, and 608 (Fig. 8a and b). The mode of interaction between givinostat and HDAC7 was mainly hydrophobic with only a single hydrogen bond formed with THR591 (Fig. 7a). However, only a single hydrogen bond was formed between betulinic acid and HDAC7 (Fig. 7b). For genistin, 5 hydrogens were formed with amino acid residues in the binding site of HDAC7 in addition to a π-alkyl interaction

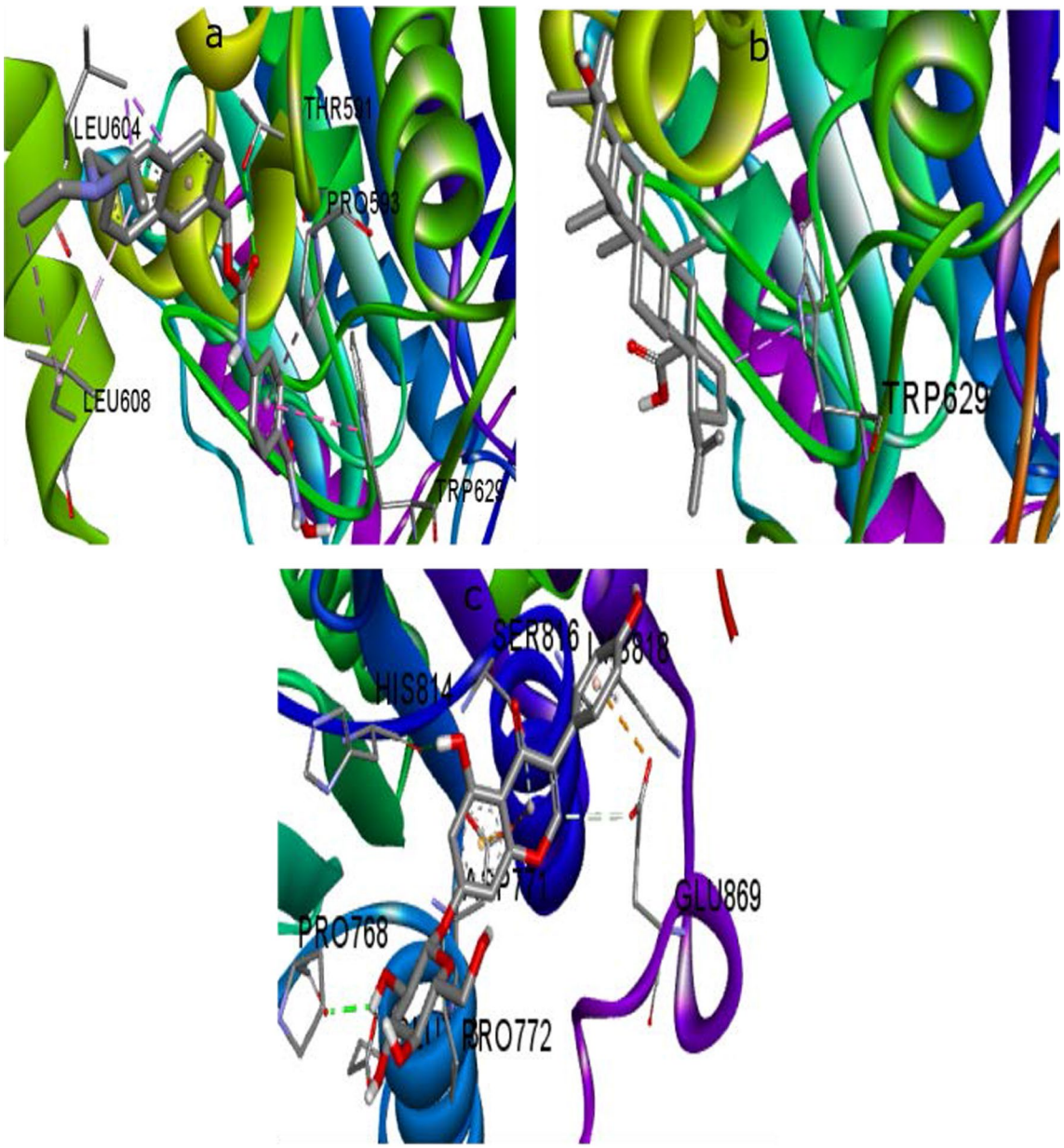

Fig. 8 3D view of the interaction between **a** givinostat **b** betulinic acid **c** genistin and the binding sites in histone deacetylase 7

with LYS818 and π-cation interaction with ASP771 and GLU869 (Fig. 7c).

The MD simulations of HDAC1, HDAC3, HDAC8, and HDAC7. All the trajectories were analyzed to understand the stability and the fluctuations of these complex structures through RMSD, RMSF, RG and MM-PBSA calculations. For HDAC1, all complexes recorded a low RMSD compared to native HDAC1. However, more stability was observed towards the last 2 ns for the test compounds compared to HDAC1-givinostat complex (Fig. 9a). For HDAC3, a relative stability was observed as from 3 ns to the end of the simulation with the exception of HDAC3-betulinic acid complex where a spike in RMSD at 6 ns (Fig. 9b). HDAC8-givinostat, HDAC8-betulinic acid and HDAC8-orientin

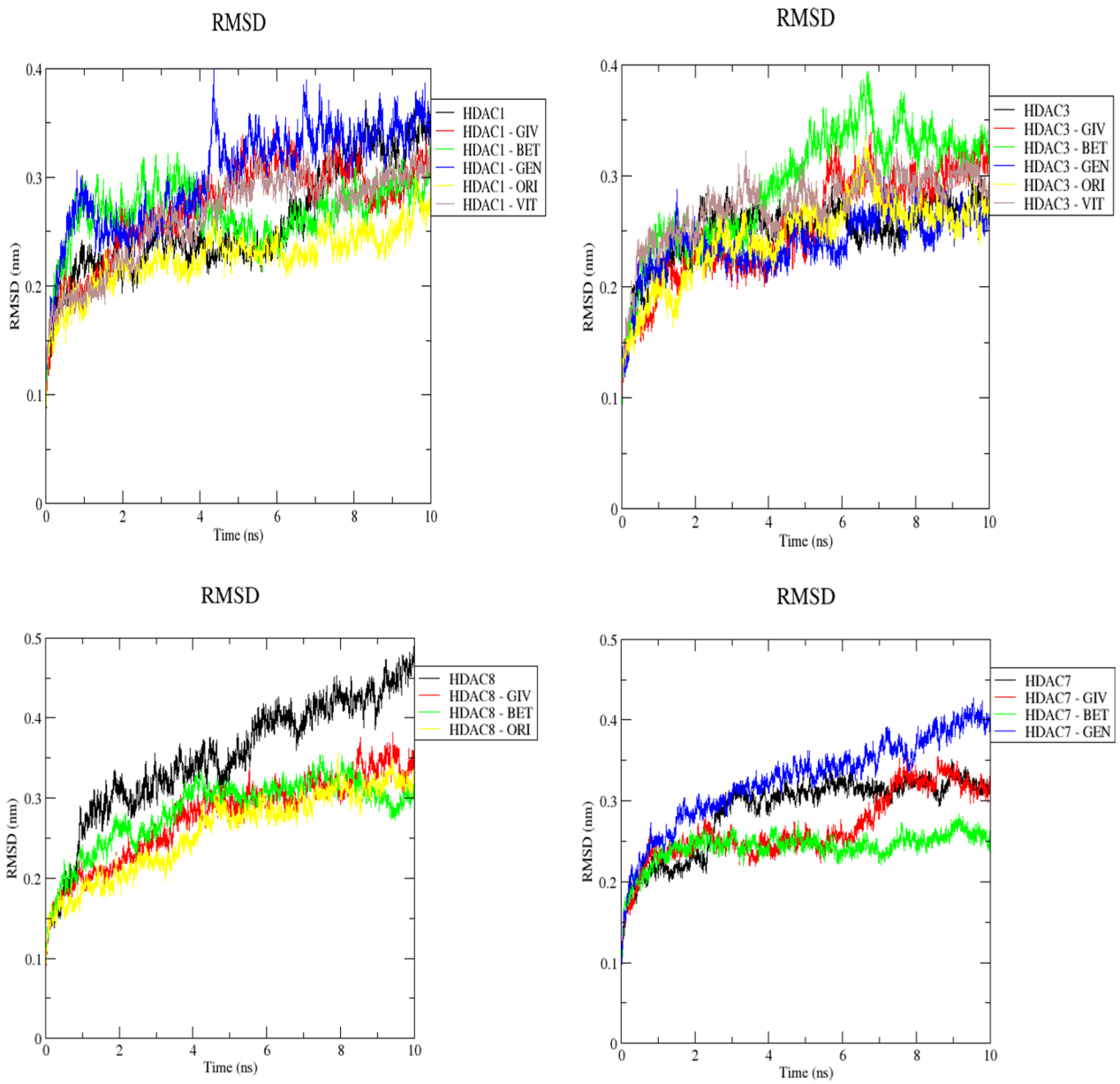

Fig. 9 RMSD study plot of HDAC1, HDAC3, HDAC8 and HDAC7 complexes during 10 ns of MD simulations

were relatively stable during the last 6 ns of simulation (Fig. 9c). HDAC7-betulinic acid with an average RMSD of 0.23 nm (Table 2) showed more stability during simulation compared to HDAC7-givinostat complex (Fig. 9d).

RMSF specifies flexible region of the protein and analyzes the regions of structures that fluctuate with regards to the overall structure. A higher RMSF value suggests greater flexibility during the MD simulation, while the lower value of RMSF indicates the system's good stability. HDAC1-complexes showed fluctuations around Arg8, Pro81-Glu86, Gly202, Asp230, Asp264 and Ala376 (Fig. 10a). Similarly, slight fluctuations were observed around His27, Thr82, Tyr207, Phe269 and Asn350 (Fig. 10b). For HDAC8 complexes, significant fluctuations were observed around Leu14, residues

Table 2 The average values of RMSD, RMSF, RG, SASA, H-Bond and Gibbs Energy of HDAC complexes

S/N	Complex	Average RMSD (nm)	Average RMSF (nm)	Average Rg (nm)	Average SASA (nm^2)	H-bond
1	HDAC1	0.33 ± 0.04	0.20 ± 0.02	2.03 ± 0.07	183.15 ± 6.32	–
2	HDAC1-Givinostat	0.35 ± 0.12	0.23 ± 0.05	2.07 ± 0.09	183.87 ± 4.13	2
3	HDAC1-Betulinic acid	0.31 ± 0.01	0.21 ± 0.01	2.04 ± 0.02	185.02 ± 2.18	1
4	HDAC1-Genistin	0.37 ± 0.09	0.24 ± 0.08	2.09 ± 0.01	172.07 ± 4.11	5
5	HDAC1-Orientin	0.26 ± 0.02	0.21 ± 0.04	2.02 ± 0.03	171.64 ± 3.95	4
6	HDAC1-Vitexin	0.30 ± 0.05	0.26 ± 0.07	2.06 ± 0.07	188.27 ± 4.39	4
7	HDAC3	0.25 ± 0.07	0.36 ± 0.05	2.02 ± 0.01	176.25 ± 3.54	–
8	HDAC3-Givinostat	0.28 ± 0.03	0.29 ± 0.02	2.05 ± 0.01	183.41 ± 6.24	3
9	HDAC3-Betulinic acid	0.37 ± 0.04	0.49 ± 0.03	2.06 ± 0.03	178.37 ± 5.08	1
10	HDAC3-Genistin	0.24 ± 0.01	0.31 ± 0.02	1.98 ± 0.04	175.28 ± 5.22	1
11	HDAC3-Orientin	0.27 ± 0.03	0.37 ± 0.06	2.00 ± 0.01	162.11 ± 7.37	3
12	HDAC3-Vitexin	0.29 ± 0.07	0.21 ± 0.03	2.04 ± 0.07	181.24 ± 4.33	4
13	HDAC8	0.42 ± 0.01	0.32 ± 0.05	2.06 ± 0.03	174.22 ± 8.15	–
14	HDAC8-Givinostat	0.29 ± 0.04	0.21 ± 0.01	2.00 ± 0.01	165.41 ± 4.58	3
15	HDAC8-Betulinic acid	0.23 ± 0.04	0.35 ± 0.03	2.02 ± 0.07	177.63 ± 7.12	1
16	HDAC8-Orientin	0.21 ± 0.06	0.38 ± 0.01	2.03 ± 0.02	170.98 ± 5.32	5
17	HDAC7	0.27 ± 0.02	0.35 ± 0.03	1.93 ± 0.11	65.23 ± 2.87	–
18	HDAC7-Givinostat	0.30 ± 0.01	0.33 ± 0.02	1.96 ± 0.08	164.22 ± 4.19	5
19	HDAC7-Betulinic acid	0.23 ± 0.04	0.37 ± 0.05	1.91 ± 0.10	157.17 ± 6.02	2
20	HDAC7-Orientin	0.38 ± 0.02	0.32 ± 0.01	1.95 ± 0.13	156.11 ± 4.12	5

between position 76 and 87 and Ala266 for HDAC8-orientin complex (Fig. 10c). HDAC7 complexes showed fluctuations at Met528, Leu555, His 581, Val621- Val 623, Phe650, while HDAC7-givinostat fluctuated significantly between Asp733-Phe738 in addition to moderate fluctuations at Gly811 and Asp865 (Fig. 10d).

The average radius of gyration (Rg) values obtained for HDAC1 complexes (Table 2) were relatively similar to those obtained for native HDAC1 (Fig. 11a). Also, HDAC3 complexes were relatively stable over the simulation period compared to native HDAC3 (Fig. 11b). HDAC8-givinostat, HDAC8-betulinic acid, HDAC8-orientin had a lower Rg compared to native HDAC8 and were all relatively stable over time (Fig. 11c). Of the four HDACs, HDAC7-complexes elicited the lowest Rg (Table 2). HDAC7-betulinic acid and HDAC7-genistin were relatively more stable compared to HDAC7-givinostat (Fig. 11d). HDAC1-genistin, HDAC1-orientin and HDAC1-vitexin had 5,4, 4 hydrogen bonds respectively Table 2). The number of hydrogen bonds in HDAC3-orientin, HDAC3-vitexin (3 and 4 respectively) is comparable to the reference (HDAC3-givinostat). HDAC8-orientin had the highest number of hydrogen bonds (5) compared to HDAC8-givinostat. Equal number of hydrogen bonds was formed in givinostat and genistin complex with HDAC7 (Fig. 12). For all class I HDACs studied i.e. HDAC1, HDAC3, and HDAC8, a significant solvent accessible surface area (SASA) was recorded (Figs. 13a, b and c). However, HDAC7-givinostat, HDAC7-betulinic acid, HDAC7-genistin had a higher SASA compared to native HDAC7 (Fig. 13d).

HDAC1 complexes exhibited a relatively lower binding energy (Table 3) during the 10 ns simulation. Also, HDAC3 complexes with the exception of HDAC3-Genistin had a lower binding energy compared to HDAC3-givinostats's -86.82 KJ mol^{-1}.

The structures of the 4 compounds with equal or higher binding affinity for HDACs 1, 3, 8 and 7 are shown in Fig. 14.

3.1 ADME study

The compounds, betulinic acid, genistin, orientin and vitexin, based on their remarkable docking properties, were considered as top compounds suitable for further studies and were therefore filtered for druglikeness. The results obtained from the ADME studies revealed that orientin violated Lipinski rule of 5 with more than 2 violations (Table 4); orientin has 11 hydrogen bond acceptor and 8 hydrogen bond donor contrary to 10

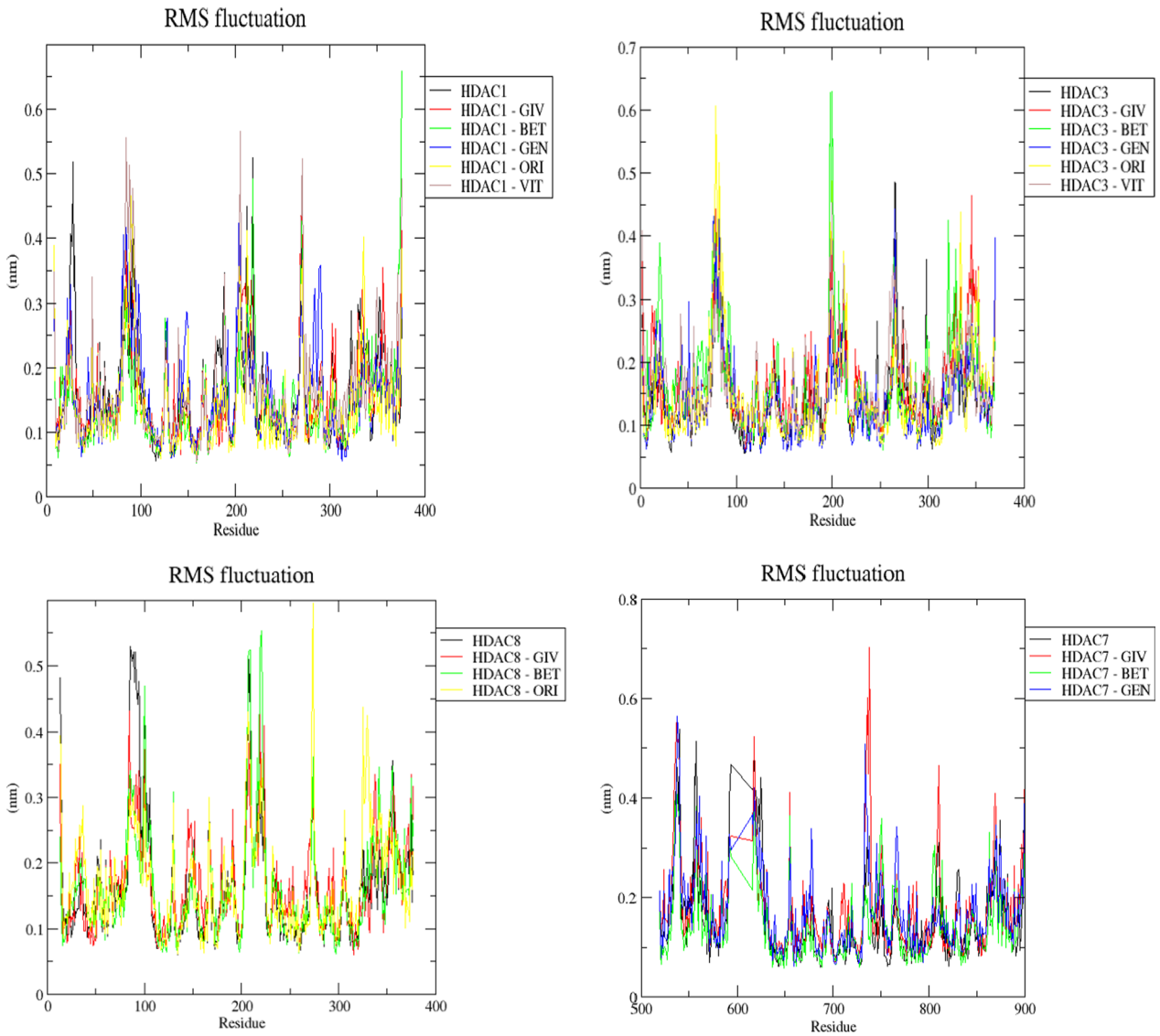

Fig. 10 The graphs reflecting the RMSF values of C-alpha atoms for HDAC1, HDAC3, HDAC8 and HDAC7 complexes

and 5 respectively as stated by Lipinski's rule. However, betulinic acid, genistin and vitexin all are within the acceptable limit of violation (i.e. one violation each).

4 Discussion

Thirteen compounds isolated from *C. cajan* have been docked with HDAC1, HDAC3, HDAC8 and HDAC7. And for comparison, the standard HDACs inhibitor, givinostat, was also docked with the selected HDACs. The goal of docking studies is to predict the binding tendency of ligands with proteins of interest in order to get useful information whether such ligands could be possible inhibitor of the target protein, and interestingly, many potential inhibitors have been identified through such in silico studies. In this current docking investigation, the phytochemical ligands with remarkable docking energies are highlighted in Table 1. Of the 13 *C. cajan* derived ligands examined, 4 compounds; betulinic acid, genistin, orientin and vitexin showed remarkable docking properties for HDAC1 and HDAC3 compared to givinostat. However, while 2 compounds (betulinic acid, and orientin) showed remarkable affinity for HDAC8, whereas 2

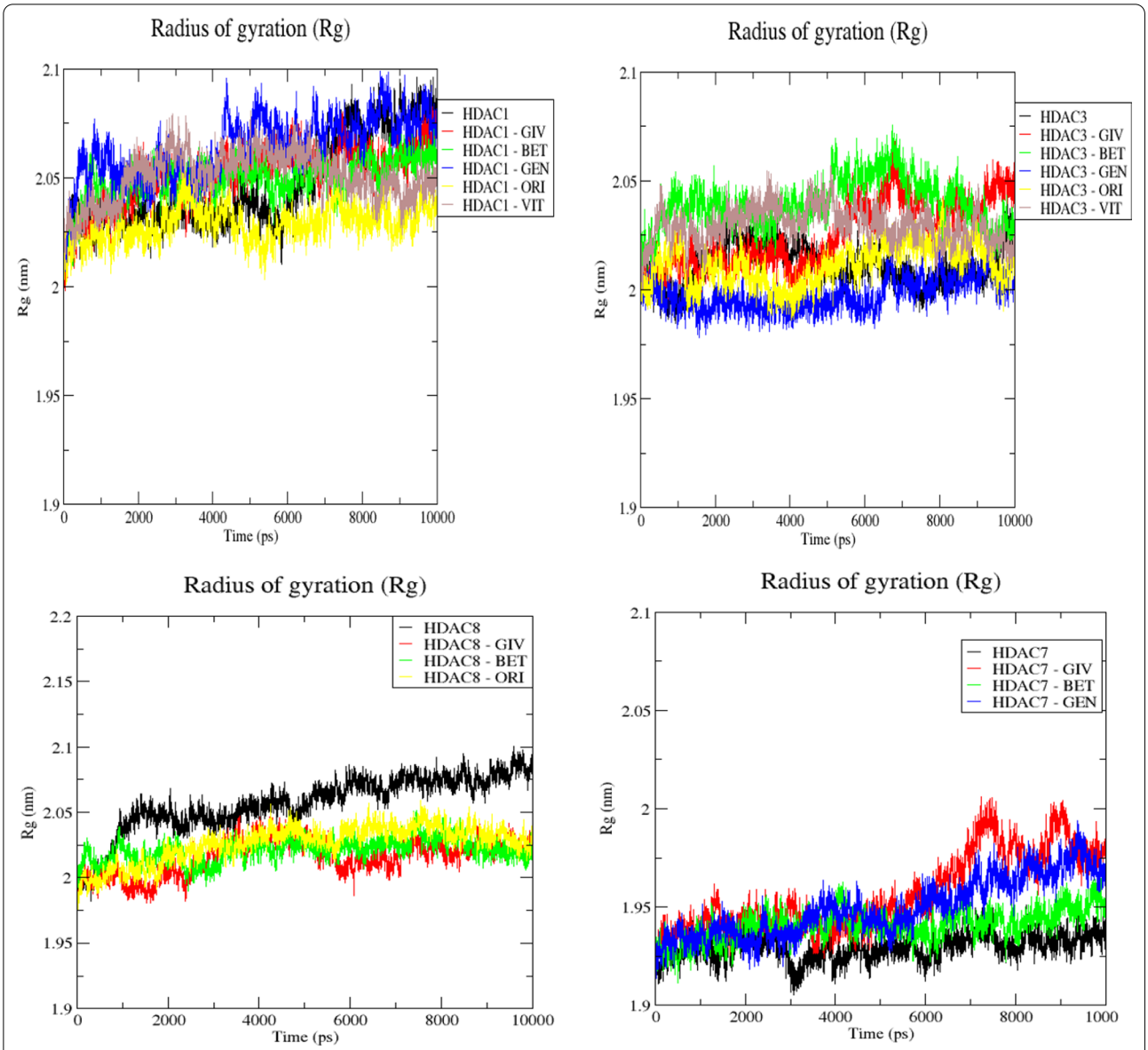

Fig. 11 Radius of gyration plots reflecting the changes observed in the conformational behavior of HDAC1, HDAC3, HDAC8 and HDAC7 complexes

compounds (betulinic acid and genistin) showed remarkable affinity for HDAC7 compared to givinostat.

Betulinic acid is a naturally occurring triterpenoid with several pharmacological activities including antiviral, antidiabetic, antihyperlipidemic, antiinflammatory and antitumor effects. The cytotoxic ability of betulinic acid on several cancer cells, such as melanoma, neuroblastoma, medulloblastoma, glioblastoma, glioma, head and neck squamous cellular, acute leukemia cells, ovarian carcinoma, colon, breast, hepatocellular, lung, prostate, renal cell and cervix carcinoma cells have been reported by several studies with the major anticancer mechanism of action being induction of direct cell death via mitochondrial apoptosis and modulation of epigenetic transcription [45–48]. In this study, results revealed that betulinic acid exhibited a higher binding tendency for all the selected HDACs relative to givinostat, and well passed Lipinski's drugability test, suggesting that betulinic acid may be a potent HDACs inhibitor and a good drug candidate for further studies on conditions associated with overexpression of these HDACs.

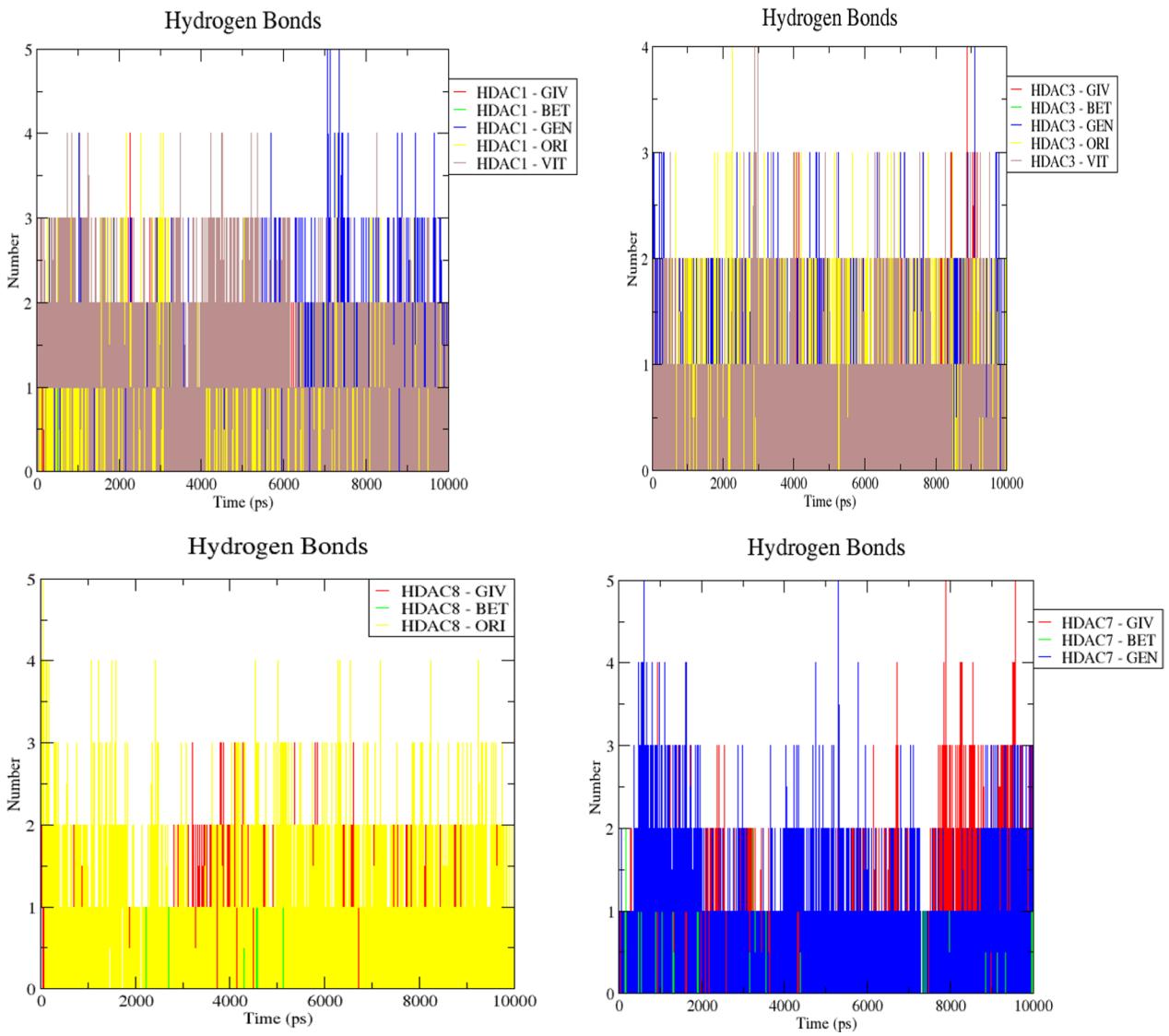

Fig. 12 The 2-D diagram describing the dynamics observed in the hydrogen bonding patterns for HDAC1, HDAC3, HDAC8 and HDAC7 complexes

Genistin is one of the popular components of soy beans, but has also been isolated in *C. cajan* [49] Tang et al. 2017; [50] Zhu et al. 2018). Genistin showed strong docking to all the selected HDACs except HDAC8. The antiproliferative capacity of this compound have been reported by many studies including breast cancer cells [50, 51] and prostate cancer cells by inducing apoptosis via increased Bax expression [52]. The results from this in silico study suggest that inhibition of HDAC may be a possible anticancer mechanism of this compound and qualifies for further studies. More so, the compound passed the Lipinski's drugability test. Orientin is a flavonoid which has been isolated from a number of plant species such as *Ficus thonningii* (Blume, Moraceae), *Ocimum sanctum* Linn. and *C. cajan* [53–55]. The antiproliferative activity of orientin against colorectal and breast carcinogenesis by modulating NF-κB mediated inflammatory response as well as suppressing MMP-9 and IL-8 expression has been reported [56, 57]. From the results obtained in this study, orientin showed strong docking to all the selected HDACs (except HDAC7), however, it violated the Lipinski rule of 5 of drug likeness. Vitexin

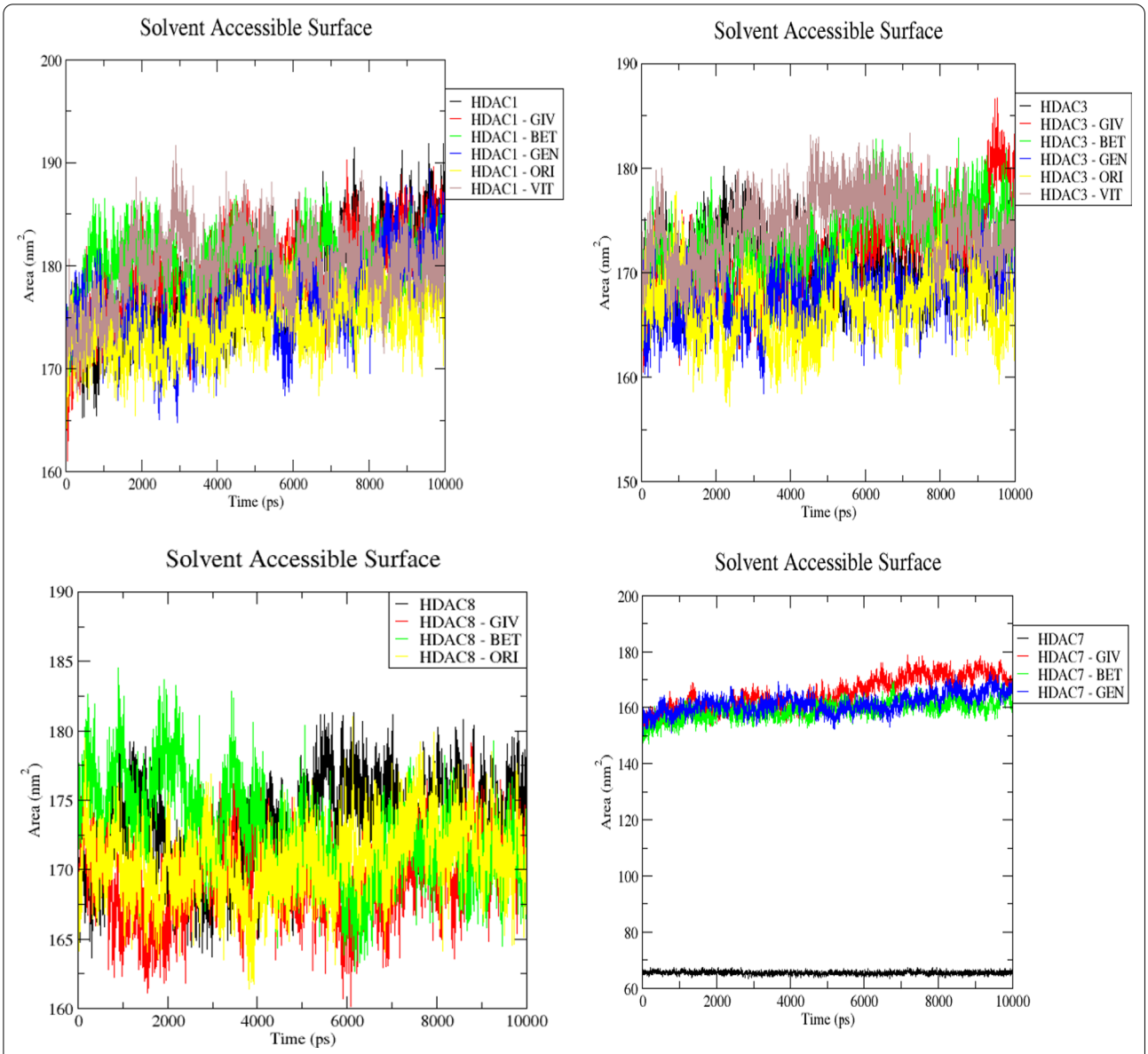

Fig. 13 Solvent accessible surface area (SASA) value vs. time at 300 K for HDAC1, HDAC3, HDAC8 and HDAC7 complexes

(apigenin-8-C-glucoside) has been found in various medicinal plants, such as pearl millet, hawthorn, mung bean, bamboo, mimosa, wheat leaves and *C. cajan*, with a range of pharmacological effects, including antioxidant, anti-inflammatory, neuroprotective and anticancer effects [58]. The reported anticancer effects are due to the promotion of apoptosis, autophagy and inhibition of proliferation and migration [58]. In this study, vitexin not only displayed remarkable binding affinity with HDAC1 and HDAC3 compared to givinostat but also passed the drugability test suggesting that this compound qualifies for further HDAC inhibitory studies using other experimental model since inhibition of HDACs might be part of the mechanisms via which this compound executes its anticancer effect.

The molecular docking study was substantiated with molecular dynamics study on the 4 HDAC targets to predict the secondary structure elements and conformational changes through the root mean square deviation and fluctuation in protein structures compared

Table 3 Binding free energies of selected protein–ligand complexes

S/N	Complex	ΔGvdw	ΔGelec	ΔGpolar sol	ΔGsasa	ΔGbind KJmol^{-1}
1	HDAC1-Givinostat	−43.22 ± 1.11	−10.19 ± 2.17	50.27 ± 3.14	−17.27 ± 1.02	−31.49 ± 1.21
2	HDAC1-Betulinic acid	−45.61 ± 2.10	−15.14 ± 3.22	61.33 ± 1.05	−24.32 ± 1.47	−23.74 ± 2.11
3	HDAC1-Genistin	−31.53 ± 3.11	−17.37 ± 1.15	44.59 ± 2.15	−31.52 ± 6.98	−35.83 ± 2.19
4	HDAC1-Orientin	−51.62 ± 4.20	−17.43 ± 2.01	63.12 ± 1.15	−37.10 ± 3.47	−43.03 ± 2.57
5	HDAC1-Vitexin	−45.21 ± 3.25	−21.47 ± 1.87	71.09 ± 2.47	−41.02 ± 1.28	−36.61 ± 3.21
6	HDAC3-Givinostat	−62.25 ± 2.45	−35.52 ± 2.21	52.21 ± 2.16	−41.26 ± 3.15	−86.82 ± 3.15
7	HDAC3-Betulinic acid	−52.57 ± 3.15	−42.02 ± 1.14	55.25 ± 3.14	−31.41 ± 2.14	−70.75 ± 2.05
8	HDAC3-Genistin	−63.17 ± 2.11	−42.52 ± 1.47	49.27 ± 1.14	−39.52 ± 1.59	−95.94 ± 2.45
9	HDAC3-Orientin	−72.15 ± 2.32	−46.23 ± 1.58	63.16 ± 2.28	−20.32 ± 3.47	−56.39 ± 5.20
10	HDAC3-Vitexin	−82.15 ± 4.25	−32.17 ± 2.58	89.55 ± 4.87	−10.22 ± 1.11	−34.99 ± 4.17
11	HDAC8-Givinostat	−59.32 ± 4.17	−36.26 ± 2.08	75.20 ± 3.17	−21.22 ± 3.33	−41.60 ± 4.20
12	HDAC8-Betulinic acid	−63.42 ± 2.56	−54.10 ± 3.39	85.85 ± 3.33	−19.45 ± 2.78	−51.12 ± 5.01
13	HDAC8-Orientin	−71.67 ± 2.89	−32.54 ± 4.32	79.21 ± 3.71	−27.19 ± 6.42	−52.19 ± 4.22
14	HDAC7-Givinostat	−69.23 ± 5.17	−43.87 ± 3.83	83.22 ± 2.17	−15.20 ± 5.29	−45.08 ± 4.57
15	HDAC7-Betulinic acid	−33.11 ± 4.44	−52.12 ± 3.15	89.52 ± 5.26	−34.26 ± 4.09	−29.97 ± 3.84
16	HDAC7-Genistin	−68.55 ± 6.03	−44.11 ± 4.18	91.22 ± 5.29	−24.28 ± 2.74	−45.72 ± 2.98

ΔGvdw = van der Waal energy, ΔGelec = electrostatic energy, ΔGpolar sol = polar solvation energy, ΔGsasa = solvent accessible surface area energy, ΔGbind = Binding energy

to the apo-form. By and large, the accommodation of inhibitor at HDAC catalytic sites is due to certain conformational changes in this vicinity [59, 60]. The RMSD results of HDAC1 and HDAC3 except around 4–6 ns and 4–8 ns respectively revealed less variability suggesting stable backbone [61, 62]. Interestingly, betulinic acid and orientin covered the narrow tunnel of HDAC1 while HDAC3 is spanned by genistin, orientin and vitexin. This pattern of conformational changes suggested a reflection of trichostatin A binding mode [63]. In addition, the RMSF results indicated that vitexin and orientin complexes fluctuate within the residues 80–92 in HDAC 1 and 3 respectively. However, between 370–380 of HDAC1 and at exactly on residue 200 in HDAC3, betulinic acid increased the fluctuation of the HDACs compared to their respective apo-forms. The observed HDAC8 fluctuation as revealed in the HDAC8 complexes RMSF values within 210–220 and 273–275 due to betulinic acid and orientin interactions respectively suggested flexibility in these regions [64]. The Rg is an effective parameter to understand the level of compactness in the structure of the protein with or without ligand indicating the folding and/or unfolding stability during the MD simulation. The HDAC7 and its complexes had the least Rg (< 1.95 nm) compared to others. Also, only the apo-HDAC8 showed higher Rg value than all its complexes indicating that the hydrophobic structure of HDAC8 was opened from the beginning to the end of the simulation. This result corresponds to the finding of Noor et al. [65] on HDAC8 stability. However, betulinic acid, orientin and vitexin increased the Rg between 6000 and 8000 ps suggesting the opening of the hydrophobic structure of HDAC3 [66]. SASA is a plot accounting for bimolecular surface area that is assessable to solvent molecules. It is evident from Fig. 13 that the observed rise in SASA values at the beginning in HDAC1 and 8; and at the end in 3 of the simulation could contribute to the stability of the complexes.

5 Conclusions

Of the 13 phytochemical ligands evaluated in this work, four compounds (betulinic acid, genistin, orientin and vitexin) showed strong docking properties to selected HDACs, compared to givinostat, the standard HDAC inhibitor besides their drug likeness properties. However, the compounds displayed considerable stability during molecular dynamics simulation with few fluctuations observed for selected residues. Therefore, the results from this in silico study provide useful structural information that can be useful in the discovery or design of HDACs inhibitors for treatment of conditions associated with their overexpression.

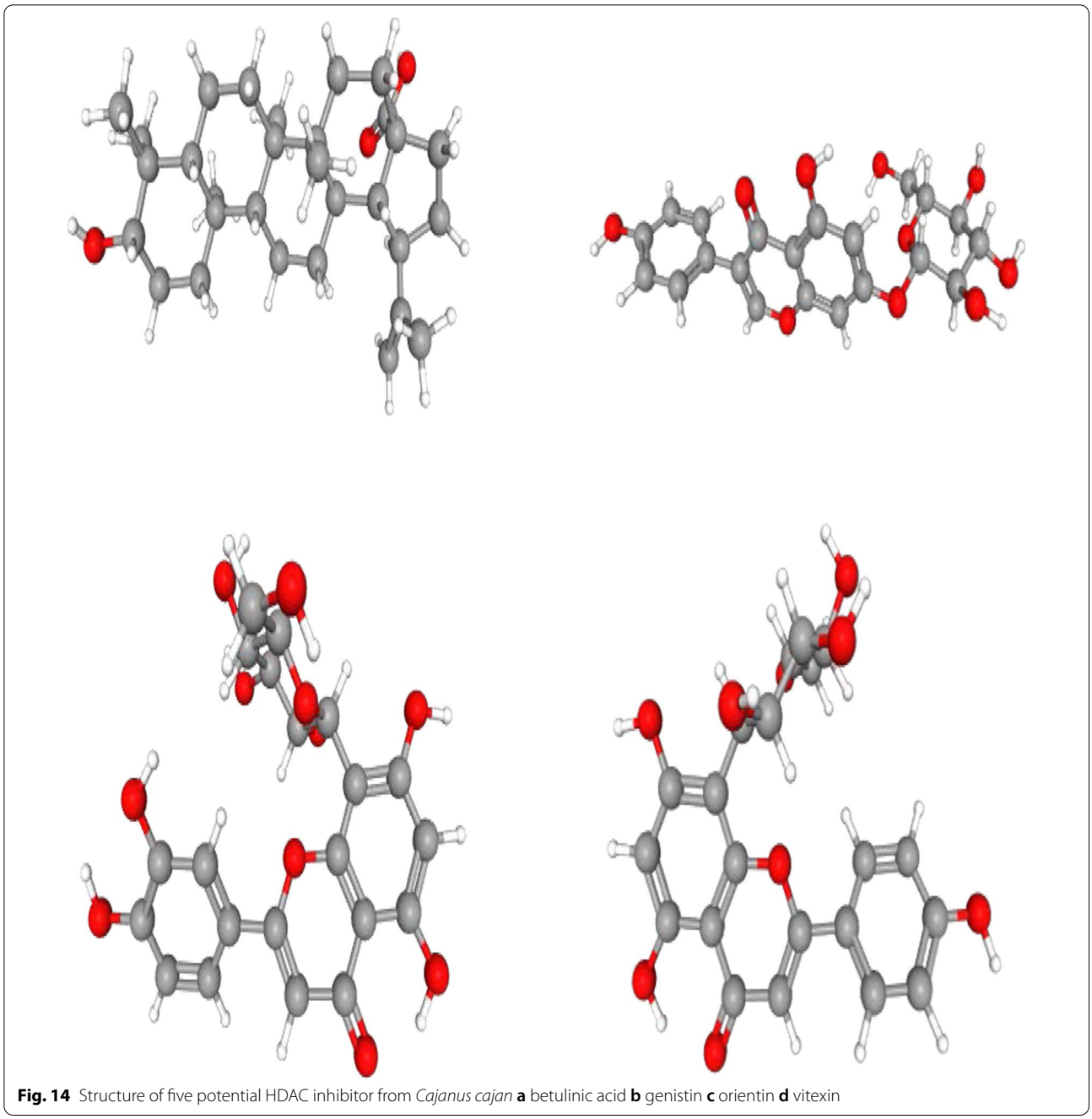

Fig. 14 Structure of five potential HDAC inhibitor from *Cajanus cajan* **a** betulinic acid **b** genistin **c** orientin **d** vitexin

Table 4 ADME properties of *Cajanus cajan* derived compounds that showed inhibitory activity HDACs

S/N	Compounds	Molecular Weight	H-bond acceptor	H-bond donor	MlogP	Rotatable bonds	Lipinski violation
1	Betulinic acid	456.7	2	3	5.82	2	1
2	Genistin	432.38	10	6	− 1.61	4	1
3	Orientin	448.38	11	8	− 2.51	3	2
4	Vitexin	432.38	10	7	− 2.02	3	1

MLOGP: octanol/water partition coefficient

Abbreviations
HDAC: Histone deacetylase; ADME: Absorption, distribution, metabolism and excretion; HDIs: HDAC inhibitors; RMSD: Root mean square deviation; RMSF: Root mean square fluctuation.

Acknowledgements
The support provided by the staff of Biochemistry Department, Faculty of Basic Medical Sciences, University of Medical Sciences, Ondo City, Ondo State, Nigeria is well appreciated.

Authors' contributions
KA and AI designed the experiment; and all authors carried out the experiment. All authors analyzed the results and wrote the manuscript. All authors read and approved the final manuscript.

Funding
This research did not receive any specific grant from funding agencies in the public, commercial, or not-for-profit sectors.

Availability of data and materials
Yes, in the main manuscript.

Declarations

Ethics approval and consent to participate
Not applicable.

Consent for publication
Not applicable.

Competing interests
On behalf of all authors, the corresponding author states that there is no conflict of interest.

Author details
[1]Department of Biochemistry, Faculty of Basic Medical Sciences, University of Medical Sciences, Ondo City, Nigeria. [2]Central Research Laboratories Limited, 132B University Road Ilorin, Ilorin, Nigeria. [3]Department of Biochemistry, McPherson University, Seriki Sotayo, Nigeria.

Received: 18 December 2020 Accepted: 23 December 2021
Published online: 10 January 2022

References

1. Díaz-de-Cerio E, Verardo V, Gómez-Caravaca A, Segura-Carretero A, Fernández-Gutiérrez A (2017) Health effects of *Psidium guajava* L. leaves: an overview of the last decade. Int J Mol Sci 18:897. https://doi.org/10.3390/ijms18040897
2. Aderinola TA, Fagbemi TN, Enujiugha VN, Monisola A, Rotimi A, Aluko E (2018) In vitro antihypertensive and antioxidative properties of derived Moringa oleifera seed globulin hydrolyzate and its membrane fractions. Food Sci Nutr 7:132–138. https://doi.org/10.1002/fsn3.826
3. Schuster R, Holzer W, Doerfler H, Weckwerth W, Viernstein H, Okonogi S, Mueller M (2016) *Cajanus cajan*—a source of PPARγ activators leading to anti-inflammatory and cytotoxic effects. Food Funct 7:3798–3806. https://doi.org/10.1039/c6fo00689b
4. Salunkhe DK, Chavan JK, Kadam SS (1986) Pigeonpea as an important food source. C R C Crit Rev Food Sci Nutr 23:103–145. https://doi.org/10.1080/10408398609527422
5. Abbiw DK (1990) Useful plants of Ghana: West African uses of wild and cultivated plants. Intermediate Technology Publications, London
6. Amalraj T, Ignacimuthu S (1998) Hypoglycemic activity of *Cajanus cajan* (seeds) in mice. Indian J Exp Biol 36:1032–1033
7. Grover JK, Yadav S, Vats V (2002) Medicinal plants of India with anti-diabetic potential. J Ethnopharmacol 81:81–100. https://doi.org/10.1016/S0378-8741(02)00059-4
8. Luo M, Liu X, Zu Y, Fu Y, Zhang S, Yao L, Efferth T (2010) Cajanol, a novel anticancer agent from Pigeonpea [*Cajanus cajan* (L.) Millsp.] roots, induces apoptosis in human breast cancer cells through a ROS-mediated mitochondrial pathway. Chem Biol Interact 188:151–160. https://doi.org/10.1016/j.cbi.2010.07.009
9. Pal D, Mishra P, Sachan N, Ghosh AK (2011) Biological activities and medicinal properties of *Cajanus cajan* (L) Millsp. J Adv Pharm Technol Res 2:207–214. https://doi.org/10.4103/2231-4040.90874
10. Fu Y, Kadioglu O, Wiench B, Wei Z, Gao C, Luo M, Gu C, Zu Y, Efferth T (2015) Cell cycle arrest and induction of apoptosis by cajanin stilbene acid from *Cajanus cajan* in breast cancer cells. Phytomedicine 22:462–468. https://doi.org/10.1016/j.phymed.2015.02.005
11. Fu Y, Kadioglu O, Wiench B, Wei Z, Wang W, Luo M, Yang X, Gu C, Zu Y, Efferth T (2015) Activity of the anti-estrogenic cajanin stilbene acid towards breast cancer. J Nutr Biochem 26:1273–1282. https://doi.org/10.1016/j.jnutbio.2015.06.004
12. Zhang N, Shen X, Jiang X, Cai J, Shen X, Hu Y, Qiu SX (2018) Two new cytotoxic stilbenoid dimers isolated from *Cajanus cajan*. J Nat Med 72:304–309. https://doi.org/10.1007/s11418-017-1138-x
13. Jeong HW, Han DC, Son KH, Han MY, Lim JS, Ha JH, Lee CW, Kim HM, Kim HC, Kwon BM (2003) Antitumor effect ofthe cinnamaldehyde derivative CB403 through the arrest of cell cycle progression in the G2/M phase. Biochem Pharmacol 65:1343–1350
14. Kaufmann SH, Hengartner MO (2001) Programmed cell death: alive and well in the new millennium. Trends Cell Biol 11:526–534
15. Houseknecht KL, Cole BM, Steele PJ (2002) Peroxisome proliferator-activated receptor gamma (PPARγ) and its ligands: A review. Domest Anim Endocrinol 22:1–23
16. Park S, Jun J, Jeong K (2011) Histone deacetylases 1, 6 and 8 are critical for invasion in breast cancer. Oncol Rep 25:677–1681
17. Barneda-zahonero B, Parra M (2012) Histone deacetylases and cancer. Mol Oncol 6:579–589. https://doi.org/10.1016/j.molonc.2012.07.003
18. Eckschlager T, Plch J, Stiborova M, Hrabeta J (2017) Histone deacetylase inhibitors as anticancer drugs. Int J Mol Sci 18:1–25. https://doi.org/10.3390/ijms18071414
19. Ropero S, Esteller M (2007) The role of histone deacetylases (HDACs) in human cancer. Mol Oncol 1:19–25. https://doi.org/10.1016/j.molonc.2007.01.001
20. Halkidou K, Gaughan L, Cook S, Leung H, Neal D, Robinson C (2004) Upregulation and nuclear recruitment of HDAC1 in hormone refractory prostate cancer. Prostate 59:177–189
21. Wilson A, Byun D, Popova N (2006) Histone deacetylase 3 (HDAC3) and other class I HDACs regulate colon cell maturation and p21 expression and are deregulated in human colon cancer. J Biol Chem 281:13548–13558
22. Huang B, Laban M, Leung C (2005) Inhibition of histone deacetylase 2 increases apoptosis and p21Cip1/WAF1 expression, independent ofhistone deacetylase 1. Cell Death Differ 12:395–404
23. Song J, Noh J, Lee J (2005) Increased expression of histone deacetylase 2 is found in human gastric cancer. APMIS 113:264–268
24. Muller BM, Jana L, Kasajinma A, Lehmann A, Prinzler J, Budczies J, Winzer K, Dietel M, Weichert W, Denkert C (2013) Differential expression of histone deacetylases HDAC1, 2 and 3 in human breast cancer-overexpression of HDAC2 and HDAC3 is associated with clinicopathological indicators of disease progression. BMC Cancer 13:215. https://doi.org/10.1186/1471-2407-13-215
25. Oehme I, Deubzer H, Wegener D (2009) Histone deacetylase 8 in neuroblastoma tumorigenesis. Clin Cancer Res 5:91–99
26. Ahn M-Y, Yoon J-H (2017) Histone deacetylase 7 silencing induces apoptosis and autophagy in salivary mucoepidermoid carcinoma cells. J Oral Pathol Med 46:276–283. https://doi.org/10.1111/ijlh.12426
27. Ganai SA, Farooq Z, Banday S, Altaf M (2018) In silico approaches for investigating the binding propensity of apigenin and luteolin against class i HDAC isoforms. Future Med Chem 10:1925–1945. https://doi.org/10.4155/fmc-2018-0020
28. Ishola A, Adewole K (2019) Phytosterols and triterpenes from Morinda lucida Benth. exhibit binding tendency against class I HDAC and HDAC7 isoforms. Mol Biol Rep 46:2307–2325. https://doi.org/10.1007/s11033-019-04689-8
29. Pandey M, Kaur P, Shukla S, Abbas A, Fu P, Gupta S (2012) Plant flavone apigenin inhibits HDAC and remodels chromatin to induce growth arrest

and apoptosis in human prostate cancer cells: in vitro and in vivo study. Mol Carcinog 51:952–962
30. Attoub S, Hassan A, Vanhoecke B (2011) Inhibition of cell survival, invasion, tumor growth and histone deacetylase activity by the dietary flavonoid luteolin in human epithelioid cancer cells. Eur J Pharmacol 651:18–25
31. Soflaei SS, Momtazi-Borojeni AA, Majeed M, Derosa G, Maffioli P, Sahebkar A (2018) Curcumin: A Natural Pan-HDAC Inhibitor in Cancer. Curr Pharm Des 24:123–129. https://doi.org/10.2174/1381612823666171114165051
32. Murugan K, Sangeetha S, Ranjitha S, Vimala A, Al-Sohaibani S, Rameshkuma G (2015) HDACiDB: a database for histone deacetylase inhibitors. Drug Des Devel Ther 9:2257–2264
33. Berman HM, Westbrook J, Feng Z, Gilliland G, Bhat TN, Weissig H, Shindyalov IN, Bourne P (2000) The protein data bank. Nucleic Acids Res 28:235–242. https://doi.org/10.1093/nar/28.1.235
34. Kim S, Chen J, Cheng T, Gindulyte A, He J, He S, Li Q, Shoemaker BA, Thiessen PA, Zaslavsky L, Zhang J, Bolton EE (2019) PubChem 2019 update: improved access to chemical data. Nucleic Acids Res 47:D1102–D1109. https://doi.org/10.1093/nar/gky1033
35. O'Boyle NM, Banck M, James CA, Morley C, Vandermeersch T, Hutchison GR (2011) Open babel: an open chemical toolbox. J Cheminform 3:33. https://doi.org/10.1186/1758-2946-3-33
36. Trott O, Olson AJ (2010) AutoDock Vina: improving the speed and accuracy of docking with a new scoring function, efficient optimization, and multithreading. J Comput Chem 31:455–461
37. Lindahl M, Abraham B, Hess D, & van der Spoel D (2021) GROMACS 2020.5 Source code, 1(6). https://doi.org/10.5281/ZENODO.4420785.
38. Hanwell MD, Curtis DE, Lonie DC, Vandermeersch T, Zurek E, Hutchison GR (2012) Avogadro: an advanced semantic chemical editor, visualization, and analysis platform. J Cheminform 4(1):17. https://doi.org/10.1186/1758-2946-4-17
39. Vanommeslaeghe K, Hatcher E, Acharya C, Kundu S, Zhong S, Shim J, Darian E, Guvench O, Lopes P, Vorobyov I, Mackerell AD Jr (2009) CHARMM general force field: a force field for drug-like molecules compatible with the CHARMM all-atom additive biological force fields. J Comput Chem 31(4):671–690
40. Kumari R, Kumar R (2014) Open source drug discovery consortium, Lynn A. g_mmpbsa—a GROMACS tool forhigh-throughput MM-PBSA calculations. J Chem Inf Model 54(7):1951–1962. https://doi.org/10.1021/ci500020m
41. Gleeson M, Hersey A, Hannongbua S (2011) In-silico ADME models: a general assessment of their utility in drug discovery applications. Curr Top Med Chem. https://doi.org/10.2174/156802611794480927
42. Daina A, Michielin O, Zoete V (2014) ILOGP: a simple, robust, and efficient description of n-octanol/water partition coefficient for drug design using the GB/SA approach. J Chem Inf Model 54:3284–3301. https://doi.org/10.1021/ci500467k
43. Daina A, Zoete V (2016) A BOILED-egg to predict gastrointestinal absorption and brain penetration of small molecules. ChemMedChem 11:1117–1121
44. Daina A, Michielin O, Zoete V (2017) SwissADME: a free web tool to evaluate pharmacokinetics, drug-likeness and medicinal chemistry friendliness of small molecules. Sci Rep 7:42717. https://doi.org/10.1038/srep42717
45. Fulda S (2009) Betulinic acid: a natural product with anticancer activity. Mol Nutr Food Res 53:140–146. https://doi.org/10.1002/mnfr.200700491
46. Ríos JL, Máñez S (2017) New pharmacological opportunities for betulinic acid authors antidiabetic properties. Planta Med 84:8–19
47. Kumar P, Bhadauria AS, Singh AK, Saha S (2018) Betulinic acid as apoptosis activator: molecular mechanisms, mathematical modeling and chemical modifications. Life Sci 209:24–33. https://doi.org/10.1016/j.lfs.2018.07.056
48. Pozas A, Reiner T, Cesare V, Trost M, Perez-stable C (2018) Inhibiting multiple deubiquitinases to reduce androgen receptor expression in prostate cancer cells. Sci Rep 8:1–16. https://doi.org/10.1038/s41598-018-31567-3
49. Tang R, Tian R, Cai J, Wu J, Shen X, Hu Y (2017) Acute and sub-chronic toxicity of *Cajanus cajan* leaf extracts. Pharm Biol 55:1740–1746. https://doi.org/10.1080/13880209.2017.1309556
50. Zhu Y, Yao Y, Shi Z, Everaert N, Ren G (2018) Synergistic effect of bioactive anticarcinogens from soybean on anti-proliferative activity in MDA-MB-231 and MCF-7 human breast cancer cells in vitro. Molecules 23:1–16. https://doi.org/10.3390/molecules23071557
51. Hamdy S, Abdel Latif A, Drees E, Soliman S (2012) Prevention of rat breast cancer by genistin and selenium genistin and selenium. Toxicol Ind Health 28:746–757. https://doi.org/10.1177/0748233711422732
52. Hsu A, Bray T, Helferich W, Doerge D, Ho E (2010) Differential effects of whole soy extract and soy isoflavones on apoptosis in prostate cancer cells. Exp Biol Med 235:90–97. https://doi.org/10.1258/ebm.2009.009128
53. Wu N, Fu K, Fu Y-J, Zu Y-G, Chang F-R, Chen Y-H, Liu X-L, Kong Y, Liu W, Gu C-B (2009) Antioxidant activities of extracts and main components of Pigeonpea [*Cajanus cajan* (L.) Millsp.] leaves. Molecules 14:1032–1043. https://doi.org/10.3390/molecules14031032
54. Dangarembizi R, Erlwanger K, Moyo D, Chivandi E (2013) Phytochemistry, pharmacology and ethnomedicinal uses of *Ficus thonningii* (Blume Moraceae): a review. Afr J Tradit Complement Altern Med 10:203–212
55. Baliga M, Rao M, Rai M, Dsouza P (2016) Radio protective effects of the Ayurvedic medicinal plant *Ocimum sanctum* Linn. (Holy Basil): a memoir. J Cancer Res Ther 12:21–27. https://doi.org/10.4103/0973-1482.151422
56. Kalaiyarasu T, Manju V (2017) Orientin, a C-glycosyl dietary flavone, suppresses colonic cell proliferation and mitigates NF-κB mediated in flammatory response in 1, 2-dimethylhydrazine induced colorectal carcinogenesis. Biomed Pharmacother 96:1253–1266. https://doi.org/10.1016/j.biopha.2017.11.088
57. Kim S, Pham T, Bak Y, Ryu H, Oh S (2018) Orientin inhibits invasion by suppressing MMP-9 and IL-8 expression via the PKC α/ERK/AP-1/STAT3-mediated signaling pathways in TPA-treated MCF-7 breast cancer cells. Phytomedicine 50:35–42. https://doi.org/10.1016/j.phymed.2018.09.172
58. He M, Min J, Kong W, He X, Li J, Peng B (2016) A review on the pharmacological effects of vitexin and isovitexin. Fitoterapia 115:74–85. https://doi.org/10.1016/j.fitote.2016.09.011
59. Park H, Lee S (2004) Homology modeling, force field design, and free energy simulation studies to optimize the activities of histone deacetylase inhibitors. J Comput Aid Mol Des 18(6):375–388
60. Yan C, Xiu Z, Li X, Li S, Hao C, Teng H (2008) Comparative molecular dynamics simulations of histone deacetylase-like protein: binding modes and free energy analysis to hydroxamic acid inhibitors. Proteins Struct Funct Bioinf 73(1):134–149
61. Martinez L (2015) Automatic identification of mobile and rigid substructures in molecular dynamics simulations and fractional structural fluctuation analysis. PLoS ONE 10(3):e0119264. https://doi.org/10.1371/journal.pone.0119264
62. Sargsyan K, Grauffel C, Lim C (2017) How molecular size impacts RMSD applications in molecular dynamics simulations. J Chem Theory Comput 13(4):1518–1524. https://doi.org/10.1021/acs.jctc.7b00028
63. Miyake Y, Keusch JJ, Wang L, Saito M, Hess D, Wang X, Melancon BJ, Helquist P, Gut H, Matthias P (2016) Structural insights into hdac6 tubulin deacetylation and its selective inhibition. Nat Chem Biol 12(9):748. https://doi.org/10.1038/nchembio.2140
64. Thangapandian S, John S, Lee KW (2012) Molecular dynamics simulation study explaining inhibitor selectivity in different class of histone deacetylases. J Biomol Struct Dyn 29(4):677–698. https://doi.org/10.1080/07391102.2012.10507409
65. Noor Z, Afzal N, Rashid S (2015) Correction: exploration of novel inhibitors for class I histone deacetylase isoforms by QSAR modeling and molecular dynamics simulation assays. PLoS ONE 10(11):e0143155. https://doi.org/10.1371/journal.pone.0143155
66. Tsukamoto S, Sakae Y, Itoh Y, Suzuki T, Okamoto Y (2018) Computational analysis for selectivity of histone deacetylase inhibitor by replica-exchange umbrella sampling molecular dynamics simulations. J Chem Phys 148(12):125102. https://doi.org/10.1063/1.5019209

Publisher's Note